Title: Lamin A/C deficiency in CD4$^+$ T-cells enhances regulatory T-cells and prevents inflammatory bowel disease.

Running Title: Lamin A/C in Treg and inflammatory bowel disease

Authors: Raquel Toribio-Fernández[a,] †, Beatriz Herrero-Fernández[b,] †, Virginia Zorita[a], Juan A. López[a,c], Jesús Vázquez[a,c], Gabriel Criado[b], Jose L. Pablos[b], Philippe Collas[d], Francisco Sánchez-Madrid[a,c,e], Vicente Andrés[a,c], Jose M. Gonzalez-Granado[a,b,c,f] *.

Affiliations:

[a]Centro Nacional de Investigaciones Cardiovasculares Carlos III (CNIC), Madrid, Spain.

[b]Instituto de Investigación Hospital 12 de Octubre (imas12), Madrid, Spain.

[c]CIBER de Enfermedades Cardiovasculares, Spain.

[d]Institute of Basic Medical Sciences, University of Oslo, Oslo, Norway.

[e]Servicio de Inmunología, Hospital de la Princesa, Instituto de Investigación Sanitaria La Princesa (IIS Princesa), Madrid, Spain.

[f]Departamento de Fisiología. Facultad de Medicina. Universidad Autónoma de Madrid (UAM), Madrid, Spain.

*Correspondence: jmgonzalez.imas12@h12o.es

Jose Maria Gonzalez Granado

Instituto de Investigación Hospital 12 de Octubre (i+12)

Hospital 12 de Octubre. Avenida de Córdoba S/N.

28041. Madrid, Spain;

Tel: +34-914531200. Fax: +34-914531265.

†Authors with equal contribution.

Conflict of interest: The authors have declared that no conflict of interests exist.

Word count: 4000

Abstract

The mechanisms by which lamin A/C in $CD4^+$ T-cells control intestinal homeostasis and can cause inflammatory bowel disease (IBD) are completely unknown. Here, we explore lamin A/C role in a mouse model of IBD. Adoptive transfer to *Rag1*$^{-/-}$ mice of *Lmna*$^{-/-}$ $CD4^+$ T-cells, which have enhanced regulatory T-cells (Treg) differentiation and function, induced less severe IBD than WT T-cells. Lamin A/C deficiency in $CD4^+$ T-cells enhanced transcription of the Treg master regulator FOXP3, thus promoting Treg differentiation, and reduced Th1 polarization, due to epigenetic changes in the Th1 master regulator T-bet. In mesenteric lymph nodes (LNs), retinoic acid (RA) released by $CD103^+$ DCs downregulated lamin A/C in $CD4^+$ T-cells, enhancing Treg differentiation. However, in peripheral LNs, non-RA-producing $CD103^-$ DCs predominate, facilitating lamin A/C expression in $CD4^+$ T-cells and therefore Th1 differentiation. Our findings establish lamin A/C as a key regulator of Th differentiation in physiological conditions and show it as a potential immune-regulatory target in IBD.

Key words: $CD4^+$ T-cells / Inflammatory Bowel Disease /FOXP3 /Lamin A-C / regulatory T-cell

Introduction

A-type lamins (lamin A/C) are type-V intermediate filaments that, together with B-type lamins, form the nuclear lamina [1,2]. Lamin A/C contributes to nuclear structure maintenance, cell migration, proliferation, differentiation, cell cycle progression, epigenetic regulation, and gene expression [3,4].

Lamin A/C is transiently expressed in $CD4^+$ T-cells upon engagement of the T-cell receptor (TCR) with an antigen; however, little is known about the function of lamin A/C in immune cells, and specifically in $CD4^+$ T-lymphocytes. $CD4^+$ T-lymphocytes are a major component of adaptive immunity, a highly complex and specialized immune response that defends against infection [5] but can also cause autoimmune diseases [6]. $CD4^+$ T-lymphocytes are activated through interaction via their TCR with an antigen in the context of MCH-II presented by an antigen-presenting cell (APC), forming a tight association called an immune synapse (IS) [7]. The transient lamin A/C expression upon antigen engagement enhances IS formation and thus $CD4^+$ T-cell activation [8].

Activated T-cells proliferate and polarize towards different phenotypes (Th1, Th2, Th17, or Treg) depending on the cytokine microenvironment and other factors [9]. The cytokine interleukin (IL-) 12 promotes Th1 polarization, inducing the transcription of Tbx21 (T-bet), whereas IL-4 enhances Th2 differentiation through the upregulation of GATA3 expression [10]. Lamin A/C significantly enhances Th1 differentiation and Th1 effector function against vaccinia virus (VACV) and *Leishmania major* infections in mice, without affecting Th2 polarization [11]. Other important T-cell phenotypes are Th17 and Tregs, which play important roles in immune-mediated inflammatory diseases [12,13]. Th17 polarization is induced by IL-23, IL-6, and TGF-β, which promote expression of the master Th17 transcription factor (TF) *Rorγt*. Treg differentiation is triggered by TGF-β and IL-2 through the induction of *Foxp3* expression [5].

Treg cells play a central role in resolving the exacerbated Th1 and Th17 proliferation and activity that causes bowel inflammation in inflammatory bowel disease (IBD), a chronic autoimmune disease of the intestine that comprises ulcerative colitis and Crohn disease [14,15]. Here, we investigated the role of lamin A/C expression in $CD4^+$ T-cells during IBD in a well-established mouse model [16,17]. In this model, adoptive transfer of WT or *Lmna*$^{-/-}$ naïve $CD4^+$ T-cells into *Rag1*$^{-/-}$ mice, which lack T-cells and B-cells, leads to bowel inflammation through the dysregulation of Th1/Treg differentiation [18-20]. Our results show that lamin A/C deficiency in $CD4^+$ T-cells protects against IBD development by reducing Th1 polarization and enhancing Treg differentiation and function, while having no effect on Th2 and Th17. Lamin A/C deficiency increased *Foxp3* expression and epigenetically decreasesreti *Tbx21* (T-bet) gene transcription, pointing to independent actions of lamin A/C in Th1 and Treg polarization. Moreover, we provide evidence that lamin A/C expression in $CD4^+$ T-cells is regulated by the differential release of retinoic acid (RA) by peripheral or mesenteric LN dendritic cells (DCs), thus determining T-cell differentiation toward the Treg or Th1 phenotype.

Materials and Methods

Detailed material and methods are described as supplementary information.

Quantitative proteomics

Proteins extraction and peptide identification were performed as described in [21] and [22], respectively. Functional protein analysis of the whole set of quantified proteins was performed using the systems biology triangle algorithm (SBT) [23].

Inflammatory bowel disease mouse model

Intestine inflammation was induced as described in [16,17]. Mice were monitored over 8 weeks to assess colitis development. Body weight and symptoms were checked twice a week. Disease severity was assigned a clinical score as follows:

- Weight loss: 0 (no loss), 1 (1–5%), 2 (5–10%), 3 (10–20%), and 4 (>20%)
- Stool consistency: 0 (normal), 2 (loose stool), and 4 (diarrhea)
- Rectal prolapse: 0 (absent), 2 (low), and 4 (pronounced)
- Rectal bleeding: 0 (absent), and 4 (present)
- Spine curvature: 0 (absent), 2 (low), and 4 (pronounced)

Histopathological analysis

Transverse colon sections (5 µm) were cut and stained with hematoxylin-eosin to evaluate inflammation severity. Images were obtained with an Olympus BX41 microscope. For each colon region, 2 images were evaluated on serial sections cut with a 100-µm separation (6 images per mouse). Colitis severity was assessed according to the following features: leukocyte infiltration, goblet cell depletion, epithelial hyperplasia, crypt damage, and submucosal inflammation, with each feature assigned a score from 0 to 4. Ulceration was also scored as follows: 0 (absent), 2 (present), and 4 (prominent). Features were scored by two blinded observers, and were summed to give a final histological score.

Chromatin immunoprecipitation-quantitative PCR

Chromatin immunoprecipitation-quantitative PCR was performed as described in [24]. Primers used for ChIP-qPCR are listed in Supplementary Table 1.

Results

Lamin A/C deficiency in CD4$^+$ T-cells enhances Treg differentiation *in vitro* by upregulating *Foxp3* transcription

Lamin A/C controls Th1 differentiation, and thus determines the immune response against infections [11]. To assess the potential role of lamin A/C in Treg and Th17 polarization, we isolated naïve CD4$^+$ T-cells from spleen and LNs of WT and *Lmna*$^{-/-}$ mice and cultured them *in vitro* with anti-CD3/CD28 antibodies plus either Treg (TGF-β and IL-2) or Th17 (IL-23 and IL-6) polarizing cytokines. *Lmna*$^{-/-}$ CD4$^+$ T-cells produced

a significantly higher proportion of Treg-cells ($CD25^+$ $FOXP3^+$) than WT cells (Figure 1A). Moreover, *Lmna*$^{-/-}$ $CD4^+$ T-cells expressed higher levels of FOXP3 than WT $CD4^+$ T-cells (Figure 1A). *Lmna*$^{-/-}$ and WT $CD4^+$ T-cells showed no significant differences in cell percentage or in mean fluorescence intensity (MFI) for the Th17 cytokine IL-17 [25] (Figure 1B). These experiments demonstrate that lamin A/C controls Treg differentiation *in vitro* by modifying *Foxp3* expression levels and suggest that lamin A/C regulates Treg differentiation upon TCR stimulation. We next analyzed the *Foxp3 and Rorc* (RORγt) mRNA expression in *Lmna*$^{-/-}$ and WT T-cells activated *in vitro* with anti-CD3/CD28 for 48 h. *Lmna*$^{-/-}$ T-cells had elevated *Foxp3* mRNA expression compared with WT controls, whereas *Rorc* (RORγt) expression did not differ between genotypes (Figure 1C). In complementary experiments, we drove increased lamin A/C in $CD4^+$ T-cells by *in vitro* transduction with GFP-lamin A/C retrovirus (Supplementary Figure 1). GFP-lamin A/C-expressing $CD4^+$ T-cells showed significantly lower Treg differentiation than GFP-expressing cells (Figure 1D), further demonstrating the role of lamin A/C in determining Treg differentiation.

Lamin A/C induces epigenetic changes in $CD4^+$ T-cells that determine Th1 commitment

To investigate the mechanism through which lamin A/C modifies Th commitment, we performed a comparative proteomic analysis between WT and *Lmna*$^{-/-}$ $CD4^+$ T-cells activated in vitro for 48 h. In a set of ~7180 analyzed proteins, 103 showed significant between-genotype differences (p-value ≤ 0.05), based on quantification with at least 2 peptides per protein and Zq values $> \pm 2$. Of these 103 proteins, 51 were upregulated and 52 downregulated in *Lmna*$^{-/-}$ $CD4^+$ T-cells. Functional analysis using the UniProt Database categorized 66 of the differentially expressed proteins into six functional groups: epigenetics, DNA machinery, immune system, metabolism, cytoskeleton, and

vesicular transport (Figure 2A). The categories with the highest numbers of differentially regulated proteins were epigenetics (16 proteins) and DNA machinery (15 proteins) (Figure 2A). This suggests that lamin A/C directly or indirectly regulates the expression of several enzymes involved in epigenetic and transcriptional processes in $CD4^+$ T-cells. Epigenetic-modifying enzymes in the epigenetic category included two components of the polycomb group (PcG) of proteins (EZH1, EED), two histone methyltransferases (CARM1, and ASH2L), two histone acetyltransferases (B2RRD7 and EP300), and two histone demethylases (PHF8 and KDM5B) (UniProt Database) (Figure 2B). Other proteins in the epigenetic category included MBD3, a protein that binds to methyl-CpG domains (UniProt Database), and LAP2α, a lamin A/C binding partner of in the nucleoplasm [26], both of which were upregulated in *Lmna*$^{-/-}$ $CD4^+$ T-cells (Figure 2B). Epigenetic regulation is a key determinant of Th fate [27], and lamin A/C is an important epigenetic modulator of cell differentiation [28,29]. We therefore investigated the capacity of lamin A/C to modulate epigenetic modifications of the master TFs of Th polarization. For this, we analyzed posttranslational histone modifications on the promoters of genes encoding these TFs in *in vitro*-activated *Lmna*$^{-/-}$ and WT $CD4^+$ T-cells. Chromatin immunoprecipitation (ChIP)-qPCR analysis of the *Foxp3* and *Rorc* (RORγt) promoters revealed no between-genotype differences for any of the modifications studied (H3K4me3, a marker of active promoters; H3K27me3 a Polycomb marker of repressed or poised promoters; and H3K4me1, an enhancer marker) (Figure 2C). In contrast, *Lmna*$^{-/-}$ T-cells had significantly fewer H3K4me1 marks on the *Tbet* promoter than WT cells (Figure 2C). As previously mentioned, *Lmna*$^{-/-}$ $CD4^+$ T-cells show different amount of EZH1 and EED (Figure 2B), components of the polycomb complex PRC2 [30,31]. To assess the role of EZH1 and EED in lamin A/C effect on epigenetic regulation, we drove reduced EZH1 and EED, by *in vitro* transduction with

EZH1 or EED RNAi retrovirus (Supplementary Figure 2) in Th1 differentiating WT and *Lmna*$^{-/-}$ CD4^{+} T-cells. EZH1, but not EED, downregulation not only abolished *Tbx21* (T-bet) mRNA differences between WT and *Lmna*$^{-/-}$ CD4^{+} T-cells but also abolished the differences in T-bet regulated-*Ifng* (IFNγ) mRNA (Figure 2D). This suggests that lamin A/C contributes to the regulation of T-bet expression during Th1 commitment, at least in part through an epigenetic mechanism.

Lamin A/C deficiency in CD4^{+} T-cells confers greater Treg immunosuppressive function

We next assessed whether lamin A/C deficiency, in addition to enhancing Treg differentiation, improves Treg function. Naïve CD4^{+} CD25^{-} T-cells were isolated from *Lmna*$^{-/-}$ and WT mice and differentiated *in vitro* toward the Treg phenotype. At 5 days of differentiation, CD25^{+} Tregs were positively selected by antibody and magnetic bead binding (Figure 3A). The obtained Tregs were characterized by RT-qPCR for the expression of cytokines commonly released by Tregs (IL-10, TGF-β, and IL-35), Treg surface receptors of the CD28 family (CTLA4, ICOS, and PD-1), and other characteristic Treg surface molecules (CD25, GITR, LAG-3, and CD49b). *Il10*, *Tgfb1* (TGF-β), *Il2ra* (CD25), *Tnfrsf18* (GITR), and *Pdcd1* (PD-1) mRNA expression was significantly increased in Tregs derived from *Lmna*$^{-/-}$ T-cells (indicated as *Lmna*$^{-/-}$ Tregs) compared with cells derived from WT T-cells (indicated as WT Tregs) (Figure 3B). Additionally, *Lag3* and *Itga2* (CD49b) expression was also higher in Tregs derived from *Lmna*$^{-/-}$ T-cells, although the difference compared with WT was not significant (Figure 3B). An *in vitro* suppression assay to test the capacity of these Tregs to inhibit Th1 proliferation showed that *Lmna*$^{-/-}$ Tregs were more potent suppressors of Th1 cell proliferation than WT Tregs (Figure 3C).

To confirm these findings in FOXP3$^+$ Tregs, we crossed *Lmna*$^{-/-}$ in CD4$^+$ T-cells mice with mice expressing RFP-FOXP3. This enabled us to sort the CD4$^+$ CD25$^+$ FOXP3$^+$ population from *in vitro*-differentiated Tregs (Figure 3D) and perform *in vitro* suppression assays on Th1 cells. Flow cytometry detection of IFNγ^+ cells confirmed that FOXP3$^+$ Tregs derived from *Lmna*$^{-/-}$ CD4$^+$ T-cells have an enhanced Th1 immunosuppressive function compared with Tregs derived from WT T-cells (Figure 3E). To ascertain the importance of FOXP3 in Treg induction in *Lmna*$^{-/-}$ CD4$^+$ T-cells, we drove reduced FOXP3 by *in vitro* transduction with *Foxp3* RNAi retrovirus (Supplementary Figure 3) in Treg differentiating WT and *Lmna*$^{-/-}$ CD4$^+$ T-cells. *Foxp3* downregulation significantly reduced GITR membrane expression in WT and *Lmna*$^{-/-}$ CD4$^+$ T-cells abolishing the differences between WT and *Lmna*$^{-/-}$ CD4$^+$ T-cells (Supplementary Figure 3). This suggests that FOXP3 mediates lamin A/C-dependent modulation of Treg differentiation and function.

Lamin A/C deficiency in CD4$^+$ T-cells protects against IBD development

To assess the impact of lamin A/C deficiency on Th1/Treg differentiation *in vivo*, we analyzed several parameters to define the inflammatory process in a mouse model of IBD based on T-cell adoptive transfer to T-cell and B-cell immunodeficient *Rag1*$^{-/-}$ mice [16,17]. Weight loss and disease symptoms were monitored twice a week, and revealed that mice adoptively transferred with *Lmna*$^{-/-}$ CD4$^+$ CD25$^-$ T-cells developed a milder disease, showing less weight loss and less severe symptoms than mice adoptively transferred with WT CD4$^+$ CD25$^-$ T-cells (Figure 4A). We also assessed colon shortening, a common feature of colitis evidencing inflammation and tissue healing [32]. Mice receiving *Lmna*$^{-/-}$ T-cells showed less colon shortening than recipients of WT T-cells (Figure 4B). To assess the anti-inflammatory effect of *Lmna*$^{-/-}$ CD4$^+$ T-cells on IBD, we quantified the IBD-associated anti-inflammatory cytokine IL-10 [33-35] in mesenteric

LNs (MLNs) by flow cytometry (Figure 4C) and in colon by RT-qPCR (Figure 4D). IL-10 expression levels were higher in mice receiving *Lmna*$^{-/-}$ T-cells than in recipients of WT T-cells. Moreover, recipients of *Lmna*$^{-/-}$ T-cells had elevated MLN mRNA expression of *Il22*, a protective cytokine in this model [36-38] and depressed mRNA expression of the pro-inflammatory cytokine *Il6* [34] (Figure 4D).

Histopathological analysis on colon slices to score colitis severity considered the following features: leukocyte infiltration, goblet cell depletion, epithelial hyperplasia, crypt damage, and submucosal inflammation. Ulceration was also considered when present. Representative micrographs clearly show that colitis was milder in mice transferred with *Lmna*$^{-/-}$ CD4^{+} T-cells than in mice transferred with WT CD4^{+} T-cells, in which colon inflammation was severe (Figure 4E and Supplementary Figure 4).

Lamin A/C mediates Treg and Th1 differentiation in the IBD mouse model.

To characterize the importance of CD4^{+} T-cell-expressed lamin A/C in IBD in more detail, we analyzed Treg, Th1, and Th17 populations in MLNs and colon isolated after 8 weeks of disease development in immunodeficient *Rag1*$^{-/-}$ mice adoptively transferred with *Lmna*$^{-/-}$ or WT naïve CD4^{+} CD25^{-} T-cells. Flow cytometry analysis detected significantly more CD25^{+} FOXP3^{+} T-cells in recipients of *Lmna*$^{-/-}$ CD4^{+} CD25^{-} T-cells than in mice receiving WT CD4^{+} CD25^{-} T-cells (Figure 5A). Conversely, the absence of lamin A/C in adoptively transferred T-cells reduced the frequency of IFNγ-positive Th1 cells. In contrast, analysis of IL-17 revealed no differences in Th17 differentiation between transferred *Lmna*$^{-/-}$ and WT CD4^{+} T-cells (Figure 5A).

This pattern of Th population changes was also revealed by RT-PCR analysis of colon tissue, with *Rag1*$^{-/-}$ recipients of *Lmna*$^{-/-}$ CD4^{+} CD25^{-} T-cells having higher mRNA expression of *Foxp3, Tgfb1* (TGF-β), and *Il35* and lower expression of *Tbet*, *Ifnγ*, and *Il12* (Figure 5B). No differences were observed in expression levels of *Rorγt* and *Il17a*,

related to Th17 differentiation (Figure 5B). However, *Il23* expression levels were lower in colon o mice receiving *Lmna*$^{-/-}$ CD4^{+} CD25^{-} T-cells, although the difference did not reach statistical significance (Figure 5B).

The intestine microenvironment is particularly rich in RA, which is released by epithelial cells and DCs [39,40]. Exposure to RA during *in vitro* activation of naïve WT CD4^{+} T-cells for 48 h downregulated lamin A/C expression in activated CD4^{+} T-cells. Immunofluorescence analysis revealed a lower proportion of lamin A/C^{+} cells in the RA-exposed population (Supplementary Figure 5A), and 3D reconstructions detected less lamin A/C MFI per cell (Supplementary Figure 5B). Stimulated and Treg differentiated WT CD4^{+} T-cells show mRNA expression of α, β and γ RA receptors (*Rara, Rarb, Rarg*, respectively) (Supplementary Figure 6A). Exposure to RA receptor α or γ agonists during *in vitro* activation of naïve WT CD4^{+} T-cells for 48 h downregulated lamin A/C expression in activated CD4^{+} T-cells (Supplementary Figure 6B).

Retinoic acid-producing CD103^{+} DCs from mesenteric lymph nodes regulates lamin A/C expression in CD4^{+} T-cells.

To assess whether lamin A/C expression in CD4^{+} T-cells is physiologically regulated depending on the lymphoid organ, we determined lamin A/C protein expression by flow cytometry in spleen, MLNs, and popliteal LNs (PLNs) in response to intraperitoneal (i.p.) VACV infection (spleen and MLN analysis) or intradermal (i.d.) infection in the footpad (PLN analysis). At 6 days post-infection, lamin A/C expression was modestly increased in CD4^{+} T-cells from spleen and MLNs, compared with a much more pronounced increase in CD4^{+} T-cells from PLNs (Figure 6A).

RA is known to be produced by the CD103^{+} DCs population, mostly present in MLNs, Peyer's Patches (PPs), and intestine, whereas it is not produced by CD103^{-} DCs, which are preferentially located in spleen and peripheral LN (PeLN) [39,41,42]. To corroborate

this, we isolated $CD11c^+$ DCs from MLNs and PeLNs, and determined the proportions of $CD103^+$ and $CD103^-$ DCs. As expected, $CD103^+$ DCs were more abundant in MLNs than PeLNs (Figure 6B). We next pulsed $CD11c^+$ DCs (CD45.2) from MLNs or PeLNs with OVA and cultured them for 48 h with WT/OTII naïve $CD4^+$ T-cells from spleen (CD45.1). Flow cytometry analysis of lamin A/C levels revealed that $CD11c^+$ DCs from MLNs strongly downregulated lamin A/C expression in $CD4^+$ T-cells compared with $CD11c^+$ DCs from PeLNs (Figure 6C).

Retinoic acid and lamin A/C deficiency in $CD4^+$ T-cells enhance Treg differentiation *in vitro* and *in vivo*.

To test whether lamin A/C is involved in the effect of RA on Treg differentiation, we performed *in vitro* Treg differentiation assays with WT and *Lmna*$^{-/-}$ $CD4^+$ T-cells activated in the presence or absence of RA for 48 h. Treg-polarizing cytokines were added at 48 h and maintained until the end of the experiment. RA exposure significantly increased the proportion of Tregs ($CD25^+$ $FOXP3^+$ cells) derived from WT $CD4^+$ T-cells, reaching levels comparable to those detected upon Treg-polarization of untreated *Lmna*$^{-/-}$ $CD4^+$ T-cells; RA exposure of *Lmna*$^{-/-}$ $CD4^+$ T-cells did not further increase the proportion of derived $CD25^+$ $FOXP3^+$ cells (Supplementary Figure 7A). In addition, assessment of FOXP3 MFI per cell showed that RA exposure of WT $CD4^+$ T-cells or the lack of lamin A/C independently enhanced Treg differentiation (Supplementary Figure 7A).

To corroborate these results *in vivo*, we treated *Rag1*$^{-/-}$ mice in the IBD model with daily i.p. injections of RA during the first 2 weeks after adoptive transfer of WT or *Lmna*$^{-/-}$ $CD4^+$ T-cells (Supplementary Figure 7B). Analysis 8 weeks after adoptive cell transfer showed that RA exposure or lack of lamin A/C independently enhanced the percentage of Tregs ($CD25^+$ $FOXP3^+$ cells) and the FOXP3 expression per cell (Supplementary

Figure 7C). Furthermore, RA treatment or lack of lamin A/C also protected mice against weight loss and colon shortening in the IBD model (Supplementary Figure 7D and E).

Discussion

Our findings suggest that lamin A/C controls T-cell differentiation, through epigenetic and non-epigenetic mechanisms. Lamin A/C regulates the abundance of enzymes related to histone modifications in activated $CD4^+$ T-cells and H3K4me1 modification in the *Tbx21* (T-bet) promoter, resulting in reduced Th1 polarization in the absence of lamin A/C. Moreover, lamin A/C also regulates FOXP3 expression, reflected in increased Treg differentiation and function in *Lmna*$^{-/-}$ $CD4^+$ T-cells. It is known that FOXP3 overexpression alone induces Treg differentiation [43]. Our data show that FOXP3 downregulation abolished lamin A/C-dependent increased Treg differentiation. Lamin A/C-dependent FOXP3 regulation does not involve epigenetic changes, since WT and *Lmna*$^{-/-}$ $CD4^+$ T-cells showed no significant differences in H3K4me3, H3K27me3, or H3K4me1 modifications in the *Foxp3* promoter. FOXP3 expression can be induced by TCR activation and IL-2 signaling, promoting the binding of NFAT, CREB, AP-1, and ATF TFs to the *Foxp3* promoter [44]. TCR activation induces lamin A/C [8], and lamin A/C can interact with TFs to modulate gene expression and cell differentiation [4,45-47]. Therefore, it is possible that lamin A/C might negatively modulate the expression of other genes related to Treg differentiation, hypothesis that warrants future investigation.

Our results from the T-cell transfer IBD model corroborate our previous data regarding naïve $CD4^+$ Th1 differentiation [11] since we observed enhanced Treg and reduced Th1 polarization upon adoptive transfer of *Lmna*$^{-/-}$ naïve $CD4^+$ T-cells. Th17 polarization was unaffected, suggesting that lamin A/C specifically regulates Th1 and Treg responses, but not Th2 or Th17 responses. An altered Th17/Treg balance has been proposed as a

common mechanism in autoimmune diseases [48]; in contrast, the Th1/Treg balance has less experimental support. A possible contribution of Th1 and Tregs has been proposed in Crohn's disease [49]. Our study demonstrates the key role of Th1/Treg misbalance in IBD, and shows how Th1 and Treg populations are functionally counter-regulated by distinct mechanisms. *Lmna*$^{-/-}$ CD4^{+} T-cells protect against IBD development in mice through the simultaneous upregulation of Tregs and downregulation of Th1 cells.

IBD is a multifactorial disease that has been linked to environmental factors, genetic susceptibility, and changes in the gut microbiota [50,51]. To avoid any influence of microbiota heterogeneity, we performed our IBD experiments under cohousing conditions [52]. The protection from IBD development in *Rag1*$^{-/-}$ mice receiving lamin A/C-deficient CD4^{+} T-cells could be due to increases in Treg differentiation and function. We show that Tregs from *Lmna*$^{-/-}$ CD4^{+} T-cells express higher levels of IL-10, TGF-β, PD-1 and CD25, pointing to an enhanced suppressive function [53,54] and elevated mRNA and protein expression of GITR, a marker of active Tregs [55]; moreover, our functional analysis demonstrates that *Lmna*$^{-/-}$ CD25^{+} Treg or *Lmna*$^{-/-}$ CD25^{+} FOXP3^{+} Treg populations have a higher Th1 suppressive activity than WT cells. Thus, our results confirm that lamin A/C deficiency in CD4^{+} T-cells not only augments Treg differentiation, but also enhances Treg immunosuppressive function, leading to reduced IBD development. Previous work demonstrated the capacity of CD4^{+} CD25^{+} Tregs to block and solve the established IBD in mice [56]. In this context, our results suggest that transfer of *in vitro* polarized Tregs lacking lamin A/C expression holds promise as a cell therapy against IBD.

Little is known on the regulation of A-type lamin expression in immune cells. An RA responsive element has been described in the LMNA promoter of P19 embryonal carcinoma cells [57], and RA is known to downregulate lamin A/C expression in the

human leukemic cell line HL-60 [58] and in human monocyte-derived myeloid cells [59]. Our study shows that RA stimulation of RARα or γ downregulates antigen-recognition-induced lamin A/C expression in $CD4^+$ T-cells *in vitro*. Moreover, lamin A/C expression in $CD4^+$ T-cells depends on the specific T-cell microenvironment *in vivo*; lamin A/C is highly expressed in activated $CD4^+$ T-cells located in PLN, whereas lamin A/C expression is significantly lower in activated $CD4^+$ T-cells in MLNs and spleen. These differences are consistent with known variations in RA availability depending on the tissue microenvironment [60]. $CD103^+$ DCs in the gut, MLNs, and PPs can release RA to T-cells undergoing activation [41], whereas $CD103^-$ DCs, located mainly in PeLN and spleen, do not produce RA [42]. Accordingly, our data confirm that MLNs contain more $CD103^+$ DCs than PeLNs and MLN-derived $CD11C^+$ DCs significantly downregulate lamin A/C expression in $CD4^+$ T-cells, whereas $CD11C^+$ DCs from PeLN do not have this effect. RA exposure can also modulate DC and macrophage phenotype, and thus affect T-cell activation, differentiation, and function indirectly. Thus, high RA concentrations generate DCs with a low T-cell activation capacity, inducing $FOXP3^+$ Tregs, whereas low RA concentrations are required for optimal T-cell activation to induce effector T-cells [61]. RA may thus have a dual effect on lamin A/C expression: a direct action on the T-cell *Lmna* promoter, and an indirect action by modifying DC phenotype, determining the T-cell lamin A/C expression response upon antigen-recognition.

Several studies have reported the capacity of RA to induce Treg differentiation from naïve T-cells. For example, RA induces FOXP3 expression when added during the activation of naïve $CD4^+$ T-cells [62]. This process appears to be dependent on TGF-β expression [41,63], but it remains unclear how RA affects *Foxp3* gene expression [64,65]. Our results confirm that RA increases Treg differentiation and show that lamin A/C downregulation during $CD4^+$ T-cell activation has a similar effect. Moreover, RA and its precursor

vitamin A have been used to ameliorate colon inflammation in mouse models [66]. Our results with the IBD mouse model corroborate this effect and show the same outcome with the adoptive transfer lamin A/C-deficient $CD4^+$ T-cells. RA-based therapy would be a multi-target treatment for IBD, whereas a strategy based on lamin A/C downregulation in $CD4^+$ T-cells could specifically resolve the Th population misbalance characteristic of the disease. Retinoids are not used to treat IBD due to concerns about their efficacy/toxicity balance in this context [67]. Other current IBD therapies such as corticosteroids and immunosuppressive drugs have severe side effects [68]. Our results suggest potential for therapeutic immunotherapy based on lamin A/C downregulation in Tregs for diseases associated with a Th1/Treg misbalance such as IBD.

In summary, our data indicate that lamin A/C deficiency in $CD4^+$ T-cells protects against IBD development by reducing Th1 polarization and enhancing Treg differentiation and function, while having no effect on Th2 and Th17 commitment. Lamin A/C deficiency increased *Foxp3* expression and epigenetically reduced *Tbx21* (T-bet) gene transcription, pointing to independent actions of lamin A/C in Th1 and Treg polarization. Moreover, we provide evidence that lamin A/C expression in $CD4^+$ T-cells is regulated by the differential release of RA by peripheral or mesenteric LN DCs, thus determining T-cell differentiation toward the Treg or Th1 phenotype.

Acknowledgments

The authors thank M.J. Andrés-Manzano, A. Sørensen and K. Vekterud for technical assistance, Dr Martín-Perez, Dr. Littman and Dr. Daley for providing reagents and S. Bartlett for English editing. This study was supported by grants to PC from the Research Council of Norway, to JMG-G from ISCIII (PI14/00526; PI17/01395; CP11/00145; CPII16/00022; EuroCellNet COST Action CA15214), the Miguel Servet Program and Fundación Ramón Aréces; to VA (RD12/0042/0028 SAF2013-46663-R, SAF2016-79490-R); to FS-M (SAF2017-82886-R; ERC-2011-AdG 294340-GENTRIS, CIBER CARDIOVASCULAR, PIE 13.0004-BIOIMID and CAM-B2017/BMD-3671-INFLAMUNE), to GC and JLP (PI16/00032 and RETICs RD16/0012 RIER), and to JV (BIO2015-67580-P; PRB3, IPT17/0019 - ISCIII-SGEFI/ERDF, ProteoRed) with co-funding from the European Regional Development Fund (ERDF) "Una manera de hacer Europa". The CNIC is supported by the Instituto de Salud Carlos III (ISCIII), the Ministerio de Ciencia, Innovación y Universidades (MCNU) and the Pro CNIC Foundation, and is a Severo Ochoa Center of Excellence (SEV-2015-0505). RTF is supported by the Fundación Ramón Aréces, VZG by ISCIII, BHF by the Instituto de Investigación Hospital 12 de Octubre (i+12), and JMG-G by the ISCIII Miguel Servet Program, i+12 and Universidad Autónoma de Madrid (UAM).

Author contributions

R.T.F and B.H.F contributed equally. R.T.F. and B.H.F. designed and performed experiments, analyzed and interpreted data, and wrote the manuscript, V.Z. performed experiments, J.A.L. carried out proteomics experiments and analysis, J.V. provided scientific input and funding for proteomics studies, J.L.P and G.C. discussed and

corrected the manuscript, P.C. provided scientific input and funding for epigenetic studies and corrected the manuscript, F.S.M. and V.A. provided scientific input and acquired funding. J.M.G.G. designed experiments, analyzed and interpreted data, wrote the manuscript, supervised the project, and acquired funding. All authors revised the manuscript and approved its final version.

References

1. Dechat T, Adam SA, Taimen P, *et al.* Nuclear lamins. *Cold Spring Harb Perspect Biol* 2010; **2**: a000547.
2. Moir RD, Yoon M, Khuon S, *et al.* Nuclear lamins A and B1: different pathways of assembly during nuclear envelope formation in living cells. *J Cell Biol* 2000; **151**: 1155-1168.
3. Schirmer EC, Foisner R. Proteins that associate with lamins: many faces, many functions. *Exp Cell Res* 2007; **313**: 2167-2179.
4. Andres V, Gonzalez JM. Role of A-type lamins in signaling, transcription, and chromatin organization. *J Cell Biol* 2009; **187**: 945-957.
5. Zhu J, Yamane H, Paul WE. Differentiation of effector CD4 T cell populations (*). *Annu Rev Immunol* 2010; **28**: 445-489.
6. Tai Y, Wang Q, Korner H, *et al.* Molecular Mechanisms of T Cells Activation by Dendritic Cells in Autoimmune Diseases. *Front Pharmacol* 2018; **9**: 642.
7. Davis SJ, van der Merwe PA. The kinetic-segregation model: TCR triggering and beyond. *Nat Immunol* 2006; **7**: 803-809.

8. Gonzalez-Granado JM, Silvestre-Roig C, Rocha-Perugini V, *et al.* Nuclear envelope lamin-A couples actin dynamics with immunological synapse architecture and T cell activation. *Sci Signal* 2014; **7**: ra37.

9. Nakayama T, Yamashita M. The TCR-mediated signaling pathways that control the direction of helper T cell differentiation. *Semin Immunol* 2010; **22**: 303-309.

10. Luckheeram RV, Zhou R, Verma AD, *et al.* CD4(+)T cells: differentiation and functions. *Clin Dev Immunol* 2012; **2012**: 925135.

11. Toribio-Fernandez R, Zorita V, Rocha-Perugini V, *et al.* Lamin A/C augments Th1 differentiation and response against vaccinia virus and Leishmania major. *Cell Death Dis* 2018; **9**: 9.

12. Joller N, Lozano E, Burkett PR, *et al.* Treg cells expressing the coinhibitory molecule TIGIT selectively inhibit proinflammatory Th1 and Th17 cell responses. *Immunity* 2014; **40**: 569-581.

13. Li B, Zheng SG. How regulatory T cells sense and adapt to inflammation. *Cellular & molecular immunology* 2015; **12**: 519-520.

14. Neurath MF, Finotto S, Glimcher LH. The role of Th1/Th2 polarization in mucosal immunity. *Nat Med* 2002; **8**: 567-573.

15. Izcue A, Coombes JL, Powrie F. Regulatory T cells suppress systemic and mucosal immune activation to control intestinal inflammation. *Immunol Rev* 2006; **212**: 256-271.

16. Morrissey PJ, Charrier K, Braddy S, *et al.* CD4+ T cells that express high levels of CD45RB induce wasting disease when transferred into congenic severe combined immunodeficient mice. Disease development is prevented by cotransfer of purified CD4+ T cells. *J Exp Med* 1993; **178**: 237-244.

17. Powrie F, Leach MW, Mauze S, *et al.* Phenotypically distinct subsets of CD4+ T cells induce or protect from chronic intestinal inflammation in C. B-17 scid mice. *Int Immunol* 1993; **5**: 1461-1471.

18. Niessner M, Volk BA. Phenotypic and immunoregulatory analysis of intestinal T-cells in patients with inflammatory bowel disease: evaluation of an in vitro model. *Eur J Clin Invest* 1995; **25**: 155-164.

19. Kosiewicz MM, Nast CC, Krishnan A, *et al.* Th1-type responses mediate spontaneous ileitis in a novel murine model of Crohn's disease. *The Journal of clinical investigation* 2001; **107**: 695-702.

20. Kang SG, Piniecki RJ, Hogenesch H, *et al.* Identification of a chemokine network that recruits FoxP3(+) regulatory T cells into chronically inflamed intestine. *Gastroenterology* 2007; **132**: 966-981.

21. Gomez-Serrano M, Camafeita E, Garcia-Santos E, *et al.* Proteome-wide alterations on adipose tissue from obese patients as age-, diabetes- and gender-specific hallmarks. *Sci Rep* 2016; **6**: 25756.

22. Trevisan-Herraz M, Bagwan N, Garcia-Marques F, *et al.* SanXoT: a modular and versatile package for the quantitative analysis of high-throughput proteomics experiments. *Bioinformatics* 2019; **35**: 1594-1596.

23. Garcia-Marques F, Trevisan-Herraz M, Martinez-Martinez S, *et al.* A Novel Systems-Biology Algorithm for the Analysis of Coordinated Protein Responses Using Quantitative Proteomics. *Mol Cell Proteomics* 2016; **15**: 1740-1760.

24. Oldenburg AR, Collas P. Mapping Nuclear Lamin-Genome Interactions by Chromatin Immunoprecipitation of Nuclear Lamins. *Methods Mol Biol* 2016; **1411**: 315-324.

25. Jin W, Dong C. IL-17 cytokines in immunity and inflammation. *Emerg Microbes Infect* 2013; **2**: e60.

26. Markiewicz E, Dechat T, Foisner R, *et al.* Lamin A/C binding protein LAP2alpha is required for nuclear anchorage of retinoblastoma protein. *Mol Biol Cell* 2002; **13**: 4401-4413.

27. Morinobu A, Kanno Y, O'Shea JJ. Discrete roles for histone acetylation in human T helper 1 cell-specific gene expression. *J Biol Chem* 2004; **279**: 40640-40646.

28. Lund E, Collas P. Nuclear lamins: making contacts with promoters. *Nucleus* 2013; **4**: 424-430.

29. Ronningen T, Shah A, Oldenburg AR, *et al.* Prepatterning of differentiation-driven nuclear lamin A/C-associated chromatin domains by GlcNAcylated histone H2B. *Genome Res* 2015; **25**: 1825-1835.

30. Kouznetsova VL, Tchekanov A, Li X, *et al.* Polycomb repressive 2 complex-Molecular mechanisms of function. *Protein Sci* 2019.

31. van Mierlo G, Veenstra GJC, Vermeulen M, *et al.* The Complexity of PRC2 Subcomplexes. *Trends Cell Biol* 2019.

32. Lindebo Holm T, Poulsen SS, Markholst H, *et al.* Pharmacological Evaluation of the SCID T Cell Transfer Model of Colitis: As a Model of Crohn's Disease. *Int J Inflam* 2012; **2012**: 412178.

33. Schreiber S, Heinig T, Thiele HG, *et al.* Immunoregulatory role of interleukin 10 in patients with inflammatory bowel disease. *Gastroenterology* 1995; **108**: 1434-1444.

34. Szkaradkiewicz A, Marciniak R, Chudzicka-Strugala I, *et al.* Proinflammatory cytokines and IL-10 in inflammatory bowel disease and colorectal cancer patients. *Arch Immunol Ther Exp (Warsz)* 2009; **57**: 291-294.

35. Zhu L, Shi T, Zhong C, *et al.* IL-10 and IL-10 Receptor Mutations in Very Early Onset Inflammatory Bowel Disease. *Gastroenterology Res* 2017; **10**: 65-69.

36. Sugimoto K, Ogawa A, Mizoguchi E, *et al.* IL-22 ameliorates intestinal inflammation in a mouse model of ulcerative colitis. *The Journal of clinical investigation* 2008; **118**: 534-544.

37. Leung JM, Davenport M, Wolff MJ, *et al.* IL-22-producing CD4+ cells are depleted in actively inflamed colitis tissue. *Mucosal immunology* 2014; **7**: 124-133.

38. Mizoguchi A, Yano A, Himuro H, *et al.* Clinical importance of IL-22 cascade in IBD. *J Gastroenterol* 2018; **53**: 465-474.

39. Iwata M, Hirakiyama A, Eshima Y, *et al.* Retinoic acid imprints gut-homing specificity on T cells. *Immunity* 2004; **21**: 527-538.

40. Czarnewski P, Das S, Parigi SM, *et al.* Retinoic Acid and Its Role in Modulating Intestinal Innate Immunity. *Nutrients* 2017; **9**. E68.

41. Coombes JL, Siddiqui KR, Arancibia-Carcamo CV, *et al.* A functionally specialized population of mucosal CD103+ DCs induces Foxp3+ regulatory T cells via a TGF-beta and retinoic acid-dependent mechanism. *J Exp Med* 2007; **204**: 1757-1764.

42. Esterhazy D, Loschko J, London M, *et al.* Classical dendritic cells are required for dietary antigen-mediated induction of peripheral T(reg) cells and tolerance. *Nat Immunol* 2016; **17**: 545-555.

43. Aarts-Riemens T, Emmelot ME, Verdonck LF, *et al.* Forced overexpression of either of the two common human Foxp3 isoforms can induce regulatory T cells from CD4(+)CD25(-) cells. *Eur J Immunol* 2008; **38**: 1381-1390.

44. Merkenschlager M, von Boehmer H. PI3 kinase signalling blocks Foxp3 expression by sequestering Foxo factors. *J Exp Med* 2010; **207**: 1347-1350.

45. Gonzalez JM, Navarro-Puche A, Casar B, *et al.* Fast regulation of AP-1 activity through interaction of lamin A/C, ERK1/2, and c-Fos at the nuclear envelope. *J Cell Biol* 2008; **183**: 653-666.

46. Dreuillet C, Tillit J, Kress M, *et al.* In vivo and in vitro interaction between human transcription factor MOK2 and nuclear lamin A/C. *Nucleic Acids Res* 2002; **30**: 4634-4642.

47. Lloyd DJ, Trembath RC, Shackleton S. A novel interaction between lamin A and SREBP1: implications for partial lipodystrophy and other laminopathies. *Hum Mol Genet* 2002; **11**: 769-777.

48. Noack M, Miossec P. Th17 and regulatory T cell balance in autoimmune and inflammatory diseases. *Autoimmun Rev* 2014; **13**: 668-677.

49. Brand S. Crohn's disease: Th1, Th17 or both? The change of a paradigm: new immunological and genetic insights implicate Th17 cells in the pathogenesis of Crohn's disease. *Gut* 2009; **58**: 1152-1167.

50. Vanhove W, Nys K, Vermeire S. Therapeutic innovations in inflammatory bowel diseases. *Clin Pharmacol Ther* 2016; **99**: 49-58.

51. Young CE, Boyle FM, Mutch AJ. Are care plans suitable for the management of multiple conditions? *J Comorb* 2016; **6**: 103-113.

52. Laukens D, Brinkman BM, Raes J, *et al.* Heterogeneity of the gut microbiome in mice: guidelines for optimizing experimental design. *FEMS Microbiol Rev* 2016; **40**: 117-132.

53. Schmidt A, Oberle N, Krammer PH. Molecular mechanisms of treg-mediated T cell suppression. *Front Immunol* 2012; **3**: 51.

54. Curotto de Lafaille MA, Lino AC, Kutchukhidze N, *et al.* CD25- T cells generate CD25+Foxp3+ regulatory T cells by peripheral expansion. *J Immunol* 2004; **173**: 7259-7268.

55. Ronchetti S, Ricci E, Petrillo MG, *et al.* Glucocorticoid-induced tumour necrosis factor receptor-related protein: a key marker of functional regulatory T cells. *J Immunol Res* 2015; **2015**: 171520.

56. Uhlig HH, Coombes J, Mottet C, *et al.* Characterization of Foxp3+CD4+CD25+ and IL-10-secreting CD4+CD25+ T cells during cure of colitis. *J Immunol* 2006; **177**: 5852-5860.

57. Okumura K, Nakamachi K, Hosoe Y, *et al.* Identification of a novel retinoic acid-responsive element within the lamin A/C promoter. *Biochem Biophys Res Commun* 2000; **269**: 197-202.

58. Olins AL, Herrmann H, Lichter P, *et al.* Nuclear envelope and chromatin compositional differences comparing undifferentiated and retinoic acid- and phorbol ester-treated HL-60 cells. *Exp Cell Res* 2001; **268**: 115-127.

59. Shin JW, Spinler KR, Swift J, *et al.* Lamins regulate cell trafficking and lineage maturation of adult human hematopoietic cells. *Proc Natl Acad Sci U S A* 2013; **110**: 18892-18897.

60. Pino-Lagos K, Benson MJ, Noelle RJ. Retinoic acid in the immune system. *Ann N Y Acad Sci* 2008; **1143**: 170-187.

61. Kim CH. Host and microbial factors in regulation of T cells in the intestine. *Front Immunol* 2013; **4**: 141.

62. Sun CM, Hall JA, Blank RB, *et al.* Small intestine lamina propria dendritic cells promote de novo generation of Foxp3 T reg cells via retinoic acid. *J Exp Med* 2007; **204**: 1775-1785.

63. Mucida D, Pino-Lagos K, Kim G, *et al.* Retinoic acid can directly promote TGF-beta-mediated Foxp3(+) Treg cell conversion of naive T cells. *Immunity* 2009; **30**: 471-472; author reply 472-473.

64. Benson MJ, Pino-Lagos K, Rosemblatt M, *et al.* All-trans retinoic acid mediates enhanced T reg cell growth, differentiation, and gut homing in the face of high levels of co-stimulation. *J Exp Med* 2007; **204**: 1765-1774.

65. Mucida D, Park Y, Kim G, *et al.* Reciprocal TH17 and regulatory T cell differentiation mediated by retinoic acid. *Science* 2007; **317**: 256-260.

66. Bai A, Lu N, Guo Y, *et al.* All-trans retinoic acid down-regulates inflammatory responses by shifting the Treg/Th17 profile in human ulcerative and murine colitis. *J Leukoc Biol* 2009; **86**: 959-969.

67. David M, Hodak E, Lowe NJ. Adverse effects of retinoids. *Med Toxicol Adverse Drug Exp* 1988; **3**: 273-288.

68. Triantafillidis JK, Merikas E, Georgopoulos F. Current and emerging drugs for the treatment of inflammatory bowel disease. *Drug Des Devel Ther* 2011; **5**: 185-210.

*Cited only in supplementary materials.

*69. Sullivan T, Escalante-Alcalde D, Bhatt H, et al. Loss of A-type lamin expression compromises nuclear envelope integrity leading to muscular dystrophy. *J Cell Biol* 1999; **147**: 913-920.

* 70. Kim Y, Zheng X, Zheng Y. Proliferation and differentiation of mouse embryonic stem cells lacking all lamins. *Cell Research* 2013; **23**: 1420-1423.

*71. Onder TT, Kara N, Cherry A, et al. Chromatin-modifying enzymes as modulators of reprogramming. *Nature* 2012; **483**: 598-602.

*72. Zhou L, Lopes JE, Chong MM, et al. TGF-beta-induced Foxp3 inhibits T(H)17 cell differentiation by antagonizing RORgammat function. *Nature* 2008; **453**: 236-240.

*73. Scaffidi P, Misteli T. Lamin A-dependent misregulation of adult stem cells associated with accelerated ageing. *Nat Cell Biol* 2008; **10**: 452-459.

*74. Wigler M, Pellicer A, Silverstein S, et al. Biochemical transfer of single-copy eucaryotic genes using total cellular DNA as donor. *Cell* 1978; **14**: 725-731.

Figure legends

Figure 1. CD4$^+$ T-cells from *Lmna*$^{-/-}$ mice show enhanced *in vitro* Treg differentiation and FOXP3 expression. (A, B) Naïve CD4$^+$ T-cells were isolated from WT and *Lmna*$^{-/-}$ mouse spleens and stimulated with anti-CD3/CD28 antibodies for 5 days in the presence of cytokines to trigger **(A)** Treg differentiation (TGF-β and IL-2) **(B)** Th17 differentiation (IL-23 and IL-6). Plots and graphs show **(A)** Treg and **(B)** Th17 differentiated cells as a percentage of total CD4$^+$ T-cells (n=3-6 pools from at least 2 mice) and (**A**) FOXP3 mean fluorescence intensity (MFI) of FOXP3$^+$ CD4$^+$ T-cells and **(B)** IL-17 MFI of IL-17$^+$ CD4$^+$ T-cells (n=7, 7 pools of 2 mice). **(C)** RT-qPCR analysis of *Foxp3* and *Rorc* (Rorγt) mRNA expression in CD4$^+$ T-cells isolated from WT and *Lmna*$^{-/-}$ mouse spleens and activated *in vitro* with anti-CD3/CD28 for 48 h (n=6 mice). Data are means ± SEM of at least 3 independent experiments analyzed by unpaired Student *t*-test; *P<0.05. **(D)** Treg differentiation of splenocytes transfected with GFP-empty or GFP-lamin A/C retrovirus. Transfected WT and *Lmna*$^{-/-}$ naïve CD4$^+$ T-cells were *in vitro* cultured with cytokines to promote Treg differentiation (see Methods). Representative flow cytometry plots show the percentage of CD25$^+$ FOXP3$^+$ cells (n=6, 6 mice). Data are means ± SEM of 2 independent experiments analyzed by one-way ANOVA with the Bonferroni multiple comparison test. *P<0.05, **P<0.01;***P<0.001, ns= not significant.

Figure 2. Lamin A/C regulates epigenetic changes modulating the expression of several epigenetic enzymes and modifying H3K4me1 in the *Tbx21* (T-bet) promoter. Naïve CD4$^+$ T-cells were isolated from WT and *Lmna*$^{-/-}$ mouse spleens and LNs and stimulated with anti CD3/CD28 antibodies for 2 days. Live cells were selected by FACS for high-throughput quantitative proteomic analysis using isobaric labeling (TMT 10-Plex analysis). **(A)** Sixty-six proteins differentially expressed between *Lmna*$^{-/-}$ and WT

$CD4^+$ T-cells are shown, categorized into 6 functional groups: epigenetics, DNA machinery, immune system, metabolism, cytoskeleton, and vesicular transport. The categories with the highest number of differentially regulated proteins were epigenetics and DNA machinery. Upregulated and downregulated proteins in *Lmna*$^{-/-}$ $CD4^+$ T-cells are indicated with red and blue arrows, respectively. **(B)** Heat-map of protein abundance changes in the epigenetics category. For each protein, the gene name is shown together with the corresponding Zq values (standardized log2 ratio) on a color scale (red indicates upregulated and blue downregulated). The mean difference (Dif) between WT and *Lmna*$^{-/-}$ Zq values is shown (n=4, 4 pools of 5 mice each). **(C)** ChIP-qPCR analysis of the indicated histone modifications in the *Foxp3, Tbx21* (T-bet), and Rorc (RORγt) promoters. Data are shown as the fold change relative to WT input sample (2 pools of 4 mice each). Data are means ± SEM of 2 independent experiments analyzed by the Student *t*-test, comparing *Lmna*$^{-/-}$ *vs* WT. *P<0.05. **(D)** RT-qPCR analysis of *Tbx21* (T-bet), and *Ifng* (IFNγ) mRNA expression in $CD4^+$ T-cells isolated from WT and *Lmna*$^{-/-}$ mouse spleens, activated *in vitro* with anti-CD3/CD28 for 48 h (n=6 mice) and retroviral transduced with RNAi scramble (pLuc), RNAi against EED (pEED) or against EZH1 (pEZH1). Data are means ± SEM of 3 independent experiments analyzed by one-way ANOVA with the Bonferroni multiple comparison test. *P<0.05, **P<0.01, ns= not significant.

Figure 3. *Lmna*$^{-/-}$ Tregs have a stronger immunosuppressive action than WT Tregs. **(A)** Naïve $CD4^+$ T-cells were isolated from WT and *Lmna*$^{-/-}$ mouse spleens and stimulated with anti CD3/CD28 antibodies for 5 days in the presence of cytokines to trigger Treg differentiation. At day 5 of *in vitro* Treg differentiation, $CD25^+$ Tregs were positively selected by magnetic sorting. **(B)** RT-qPCR analysis of the indicated Treg-related genes; mRNA expression is shown as the fold change *vs* WT (n=6-9, at least 6 pools of 2 mice

each). Data are means ± SEM of 6 pools of 2 mice analyzed by unpaired Student *t*-test comparing *Lmna*$^{-/-}$ *vs* WT; *P<0.05. **(C)** Treg suppression assay with *in vitro*-differentiated CD25^{+} Tregs from CD45.2 WT and *Lmna*$^{-/-}$ mice cocultured with naïve CD4^{+} T-cells isolated from CD45.1 WT mouse spleens. For cocultures, Tregs were used at the indicated serial dilutions (1:2, 1:4, 1:8, 1:16, 1:32, 1:64, 1:0) with a constant naïve CD4^{+} T-cell concentration in the presence of IL-12, IL-2, and soluble anti-CD3/CD28 antibodies. Naïve CD4^{+} T-cells were stained with Cell Violet to quantify the T-cell proliferation rate. Representative plots of the 1:4 and 1:8 Treg dilutions are shown, and the graph shows the percentage of proliferative naïve CD4^{+} T-cells (n=4, 4 mice of a representative experiment of 2). Data are means ± SEM of 4 mice analyzed by 2-way ANOVA with the Bonferroni multiple comparison test. **(D)** At day 5 of *in vitro* Treg differentiation, FOXP3-RFP^{+} Tregs from CD4-CRE-Lmna$^{flox/flox}$-FOXP3-RFP mice were selected by FACS. **(E)** The WT and *Lmna*$^{-/-}$ FOXP3-RFP^{+} Tregs were cocultured with naïve CD4^{+} T-cells isolated from CD45.1 WT mice in the presence of IL-12, IL-2, and soluble anti-CD3/CD28 in a similar suppression assay to that described above. Representative plots are shown of the 1:8 and 1:16 Treg dilution, and the graph shows the percentage of IFNγ^{+} cells (n=3, 3 pools of 2 mice in a representative experiment of 2). Data are means ± SEM analyzed by 2-way ANOVA with the Bonferroni multiple comparison test. *P<0.05;**P<0.01;***P<0.001.

Figure 4. A-type lamin deficiency in CD4^{+} T-cells protects against IBD development in mice. *Rag1*$^{-/-}$ mice were adoptively transferred with WT or *Lmna*$^{-/-}$ CD4^{+} CD25^{-} T-cells to induce IBD. Mice were sacrificed 8 weeks after T-cell transfer. **(A)** Evolution of body weight loss and colitis symptoms during IBD development (n=6-7, at least 6 mice from a representative experiment of 5). Data are means ± SEM of at least 6 mice analyzed by 2-way ANOVA with the Bonferroni multiple comparison test. **(B)** Representative

colons and quantification of colon length (mm) after 8 weeks of IBD development (n=6-7 mice from a representative experiment). Data are means ± SEM of at least 6 mice analyzed by one-way ANOVA with the Bonferroni multiple comparison test. **(C)** IL-10^+ cells as a percentage of the total $CD4^+$ T-cell population in mesenteric LNs (MLNs) after 8 weeks of IBD development **(D)** RT-qPCR analysis of the indicated inflammation-related genes in the colon after 8 weeks of IBD development (n=7, at least 7 mice from a representative experiment of 5). Data are means ± SEM of at least 6 mice analyzed by unpaired Student *t*-test. **(E)** Representative micrographs of hematoxylin-eosin stained colon sections (scale bars, 500 µm at 4x magnification and 250 µm at 10x magnification). The graph shows the disease score (0-3) recapitulating markers of intestinal inflammation indicated on the micrograph: leukocyte infiltration (1), goblet cell depletion (2), epithelial hyperplasia (3), crypt damage (4), and submucosal inflammation (5) (n=6-7, at least 6 mice from a representative experiment of 5). Data are means ± SEM analyzed by one-way ANOVA with the Bonferroni multiple comparison test. *P<0.05;**P<0.01;***P<0.001. Black *: comparison between WT and *Lmna*$^{-/-}$. Red ***:** comparison between WT and No CD4. Blue ***:** comparison between *Lmna*$^{-/-}$ and No CD4.

Figure 5. A-type lamins mediate Treg and Th1 differentiation in the IBD mouse model. *Lmna*$^{-/-}$ and WT $CD4^+$ $CD25^-$ T-cells were adoptively transferred to *Rag1*$^{-/-}$ mice to induce IBD, assessed 8-weeks post adoptive transfer. **(A)** $CD25^+FOXP3^+$, $IFN\gamma^+$, and IL-17^+ cells as a percentage of the total $CD4^+$ T-cell population in MLNs and the colonic lamina propria (n=3 mice from a representative experiment). **(B)** RT-qPCR analysis of the indicated genes related to Treg, Th1, and Th17 differentiation in colon (n=6 mice). Data are means ± SEM of a representative experiment analyzed by unpaired Student *t*-test comparing *Lmna*$^{-/-}$ *vs* WT. *P<0.05;**P<0.01;***P<0.001.

Figure 6. An RA-producing CD103$^+$ DCs population is prominent in mesenteric lymph nodes and downregulates lamin A/C expression in CD4$^+$ T-cells. CD11c$^+$ DCs were isolated from MLNs or peripheral lymph nodes (PeLNs) of CD45.2 WT mice. **(A)** Lamin A/C mean fluorescence intensity (MFI) analysis by flow cytometry of CD4$^+$ CD69$^+$ CD25$^+$ T-cells upon intraperitoneal (spleen and MLN) and footpad (PLN) infection with vaccinia virus (n=5, 5 mice). **(B)** Representative plots showing the enrichment of MLNs for CD11c$^+$CD103$^+$ DCs *vs* PeLNs; the graph shows the percentage of CD11c$^+$ CD103$^+$ DCs in MLNs and PeLNs (n=4, 4 mice) **(C)** Coculture of OVA-loaded CD11c$^+$ DCs isolated from MLNs or PeLNs of CD45.2 WT mice with CD45.1 WT/OTII naïve CD4$^+$ T-cells from spleen. The plot and graphs show lamin A/C MFI and the percentage of lamin A/C-positive CD4$^+$ T-cells at 48 h of activation. Data are means ± SEM of a representative experiment of 3 analyzed by unpaired Student *t*-test. *P<0.05;**P<0.01.

Provided supplementary material:

Supplementary detailed material and methods

Supplementary Figures 1 to 7

Supplementary Figure legends

Supplementary Tables 1 and 2

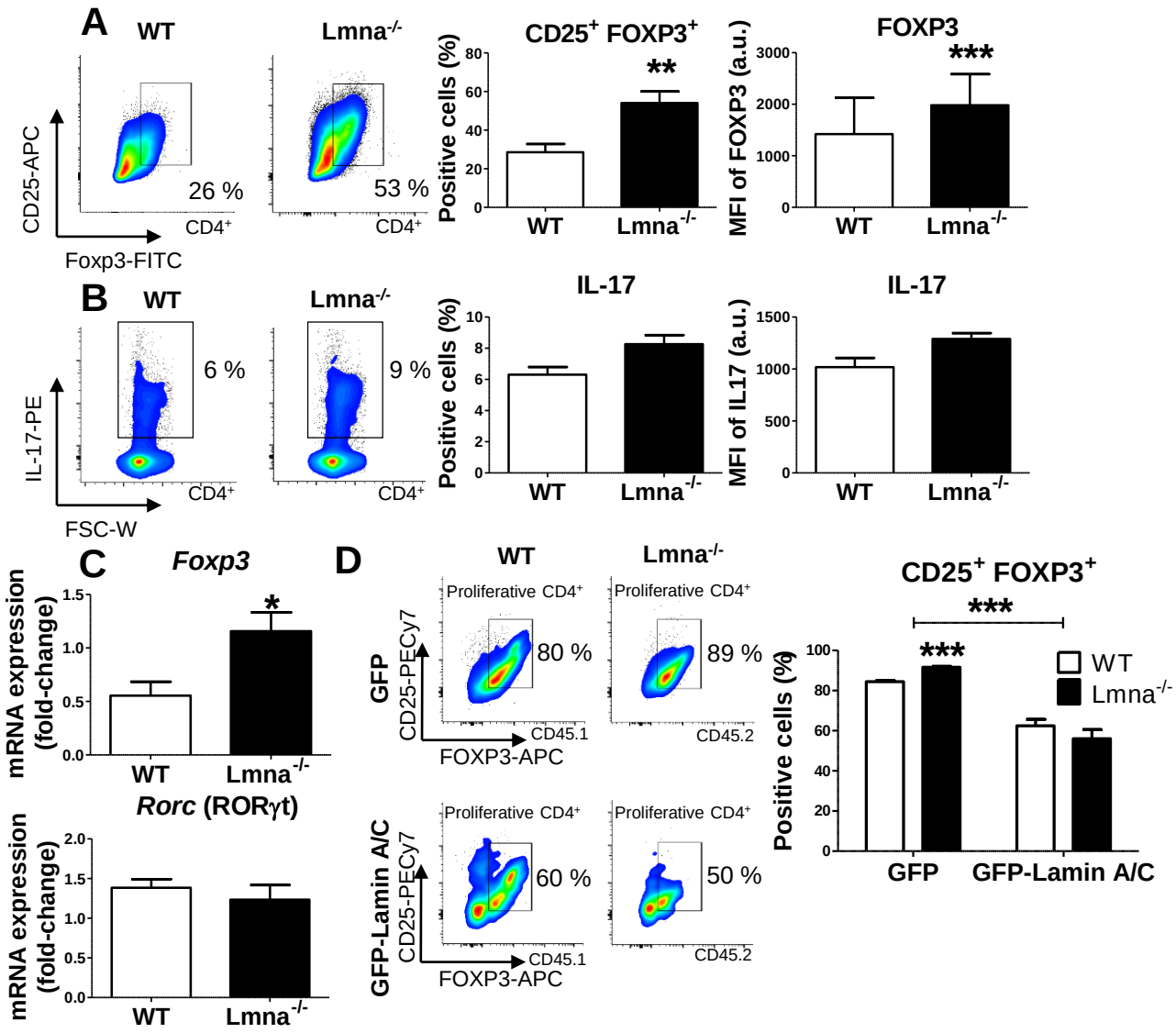
A
WT
Lmna-/-
CD25-APC
Foxp3-FITC
26 %
53 %
CD4+
CD25+ FOXP3+
Positive cells (%)
**
WT
Lmna-/-
FOXP3
MFI of FOXP3 (a.u.)
***
B
IL-17-PE
FSC-W
6 %
9 %
IL-17
MFI of IL17 (a.u.)
C
Foxp3
mRNA expression (fold-change)
*
Rorc (RORγt)
D
Proliferative CD4+
GFP
CD25-PECy7
CD45.1
CD45.2
FOXP3-APC
80 %
89 %
GFP-Lamin A/C
60 %
50 %
CD25+ FOXP3+
GFP
GFP-Lamin A/C

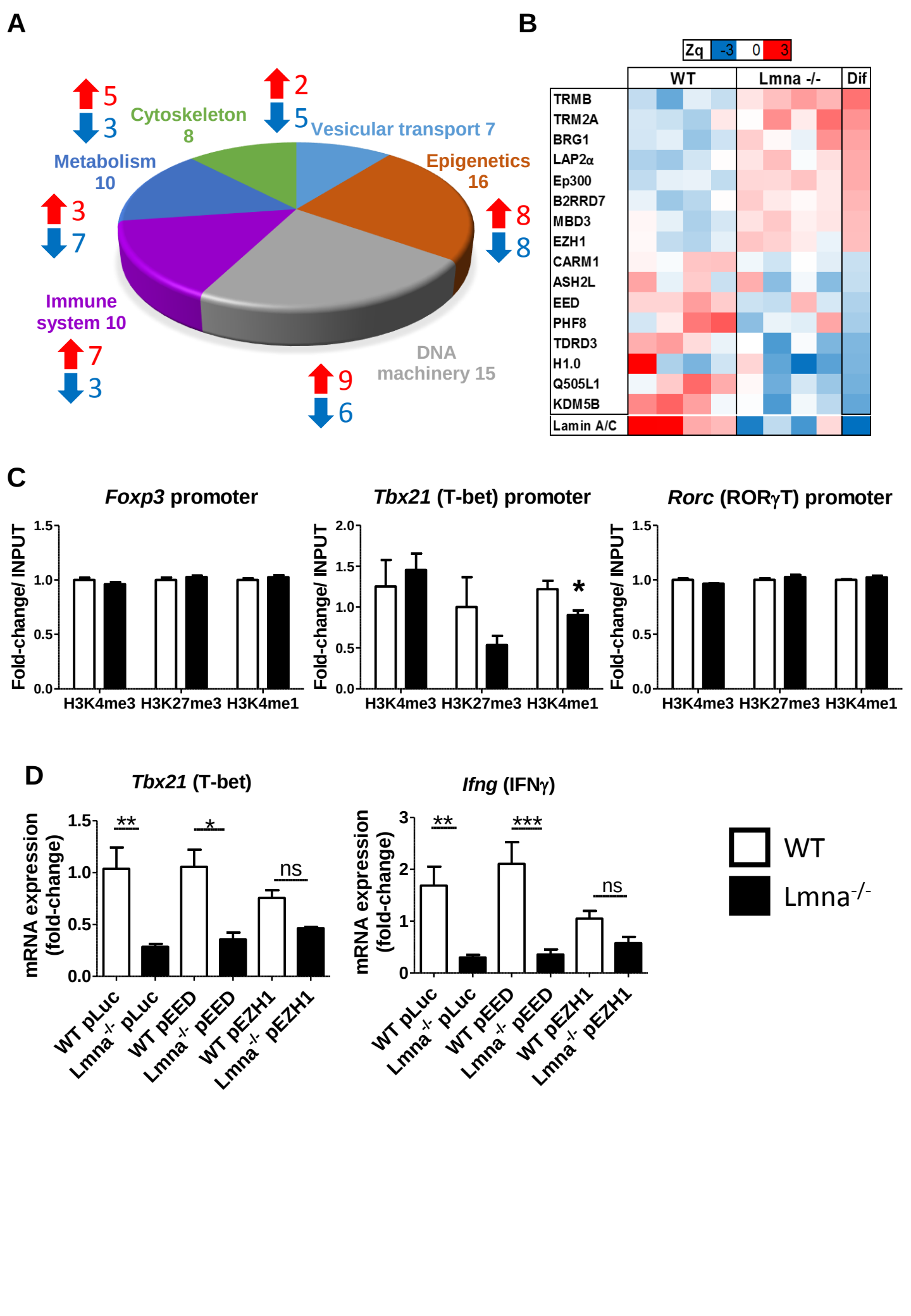
A
5
3
Cytoskeleton
8
2
5
Vesicular transport 7
Metabolism
10
Epigenetics
16
3
7
8
8
Immune
system 10
7
3
DNA
machinery 15
9
6
B
Zq
-3
0
3
WT
Lmna -/-
Dif
TRMB
TRM2A
BRG1
LAP2α
Ep300
B2RRD7
MBD3
EZH1
CARM1
ASH2L
EED
PHF8
TDRD3
H1.0
Q505L1
KDM5B
Lamin A/C
C
Foxp3 promoter
Tbx21 (T-bet) promoter
Rorc (RORγT) promoter
Fold-change/ INPUT
1.5
1.0
0.5
0.0
2.0
1.5
1.0
0.5
0.0
*
H3K4me3
H3K27me3
H3K4me1
D
Tbx21 (T-bet)
Ifng (IFNγ)
mRNA expression
(fold-change)
1.5
1.0
0.5
0.0
3
2
1
0
**
*
***
ns
WT pLuc
Lmna -/- pLuc
WT pEED
Lmna -/- pEED
WT pEZH1
Lmna -/- pEZH1
WT
Lmna-/-

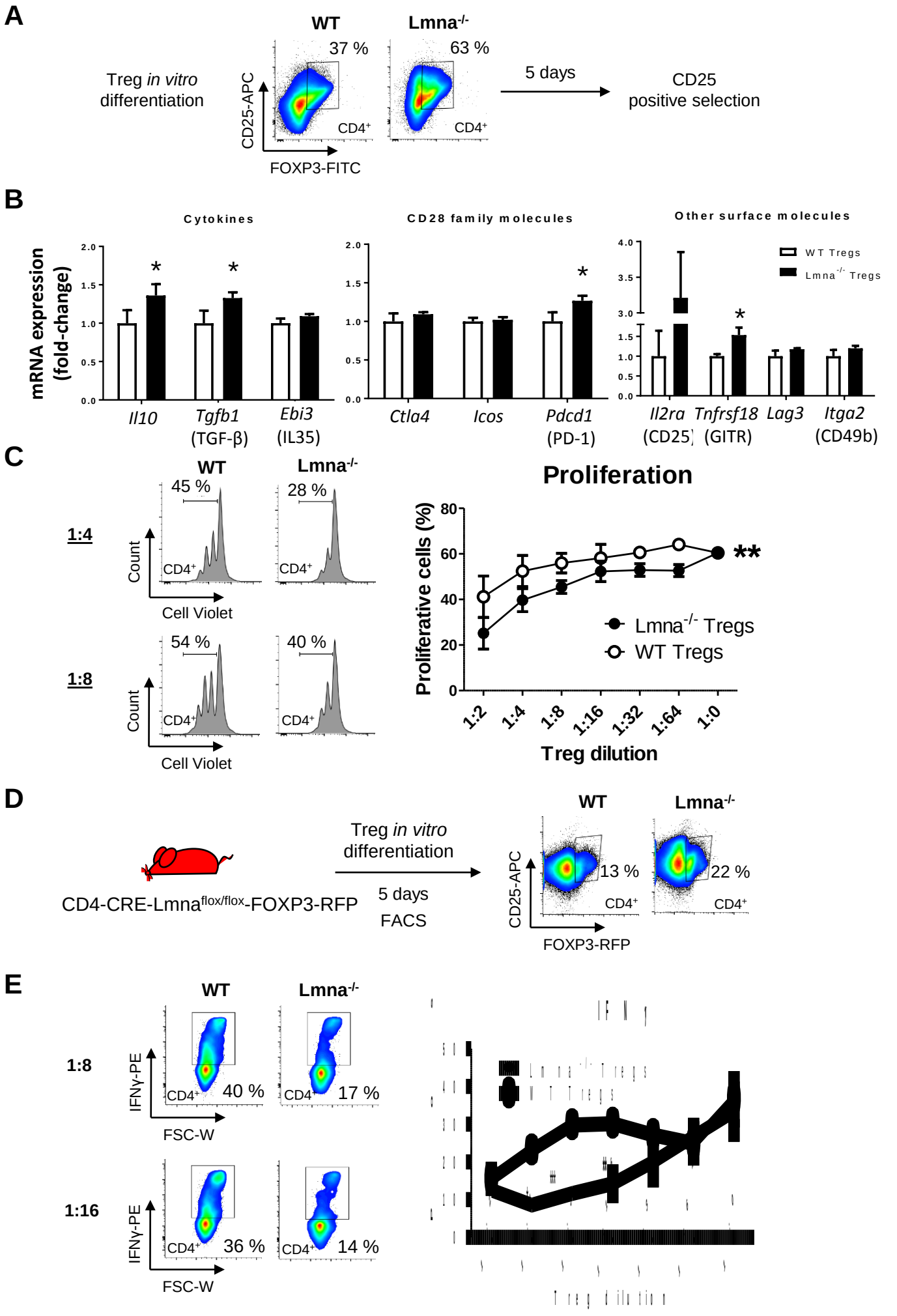
A
WT
Lmna-/-
37 %
63 %
CD4+
CD4+
CD25-APC
FOXP3-FITC
Treg in vitro differentiation
5 days
CD25 positive selection
B
Cytokines
CD28 family molecules
Other surface molecules
mRNA expression (fold-change)
WT Tregs
Lmna-/- Tregs
Il10
Tgfb1 (TGF-β)
Ebi3 (IL35)
Ctla4
Icos
Pdcd1 (PD-1)
Il2ra (CD25)
Tnfrsf18 (GITR)
Lag3
Itga2 (CD49b)
C
WT
Lmna-/-
1:4
1:8
45 %
28 %
54 %
40 %
Count
Cell Violet
Proliferation
Proliferative cells (%)
Lmna-/- Tregs
WT Tregs
Treg dilution
1:2
1:4
1:8
1:16
1:32
1:64
1:0
D
CD4-CRE-Lmnaflox/flox-FOXP3-RFP
Treg in vitro differentiation
5 days
FACS
WT
Lmna-/-
13 %
22 %
CD25-APC
FOXP3-RFP
E
WT
Lmna-/-
1:8
1:16
IFNγ-PE
FSC-W
40 %
17 %
36 %
14 %

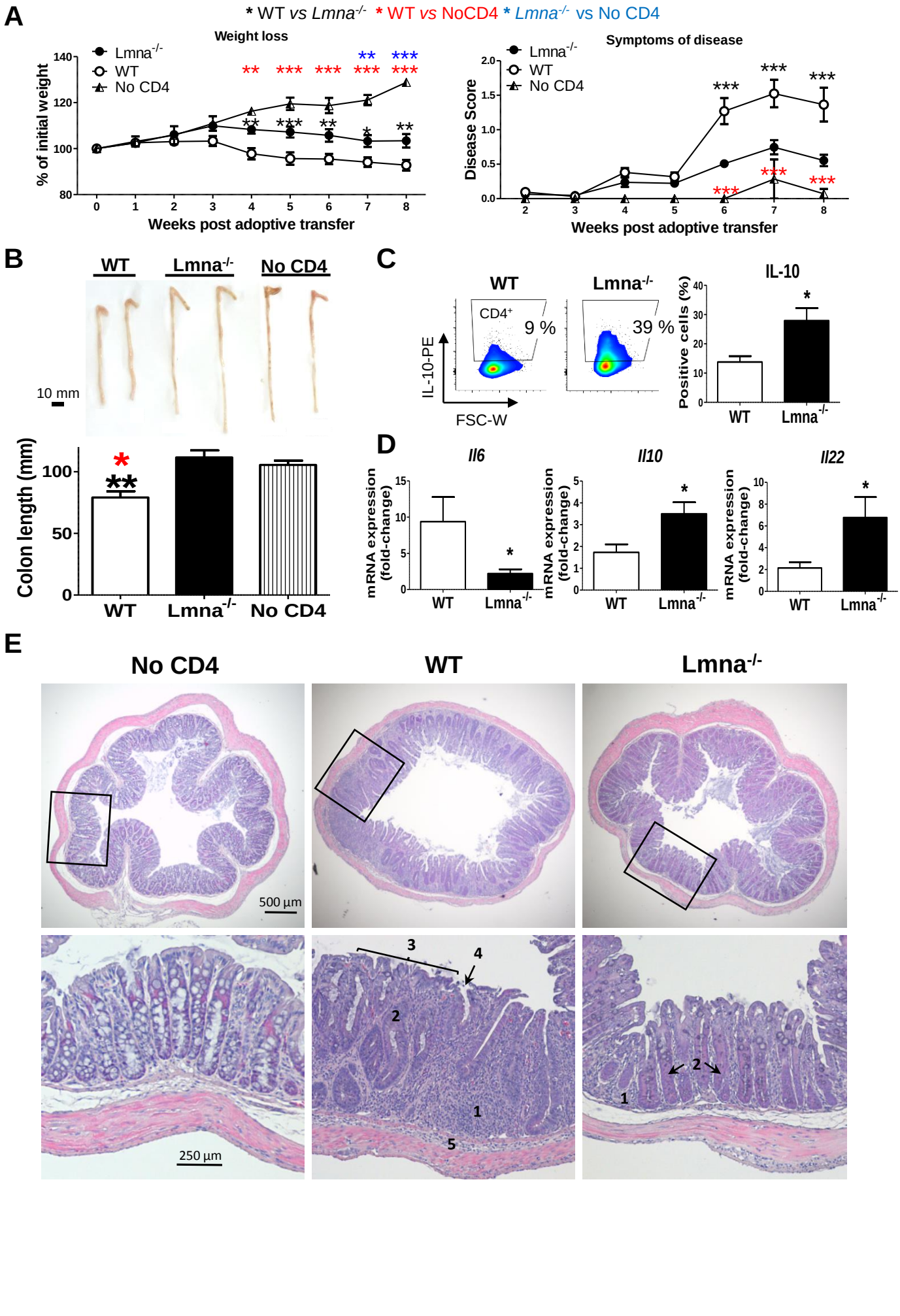
A
* WT vs Lmna-/- * WT vs NoCD4 * Lmna-/- vs No CD4
Weight loss
Lmna-/-
WT
No CD4
% of initial weight
Weeks post adoptive transfer
Symptoms of disease
Disease Score
Weeks post adoptive transfer
B
WT
Lmna-/-
No CD4
10 mm
Colon length (mm)
C
WT
Lmna-/-
CD4+
9 %
39 %
IL-10-PE
FSC-W
IL-10
Positive cells (%)
D
Il6
Il10
Il22
mRNA expression (fold-change)
E
No CD4
WT
Lmna-/-
500 µm
250 µm
1
2
3
4
5

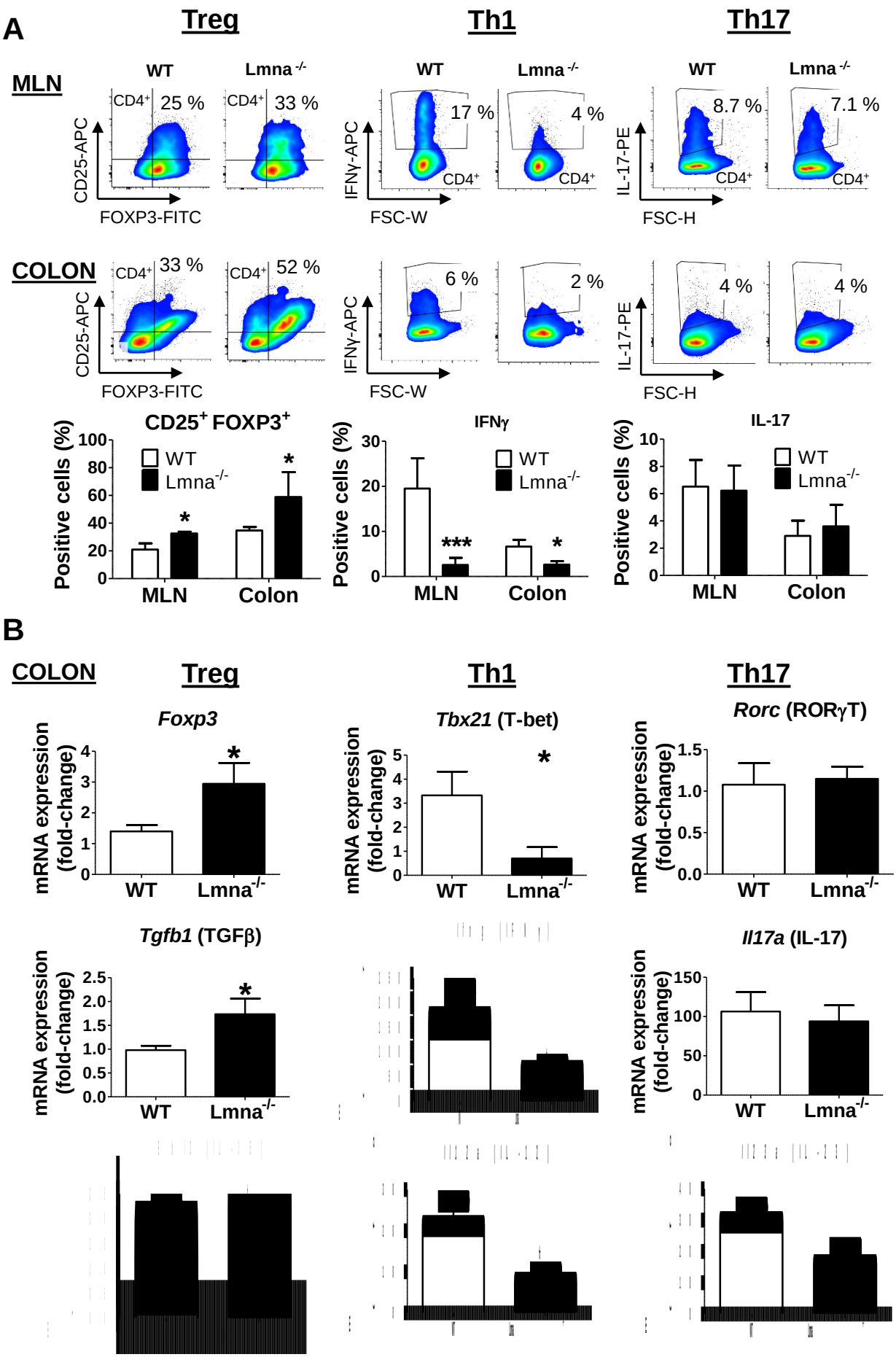
A
Treg
Th1
Th17
MLN
COLON
WT
Lmna -/-
CD4+
25 %
33 %
17 %
4 %
8.7 %
7.1 %
52 %
6 %
2 %
CD25-APC
FOXP3-FITC
IFNγ-APC
FSC-W
IL-17-PE
FSC-H
CD25+ FOXP3+
IFNγ
IL-17
Positive cells (%)
Lmna-/-
MLN
Colon
B
Foxp3
Tbx21 (T-bet)
Rorc (RORγT)
Tgfb1 (TGFβ)
Il17a (IL-17)
mRNA expression (fold-change)

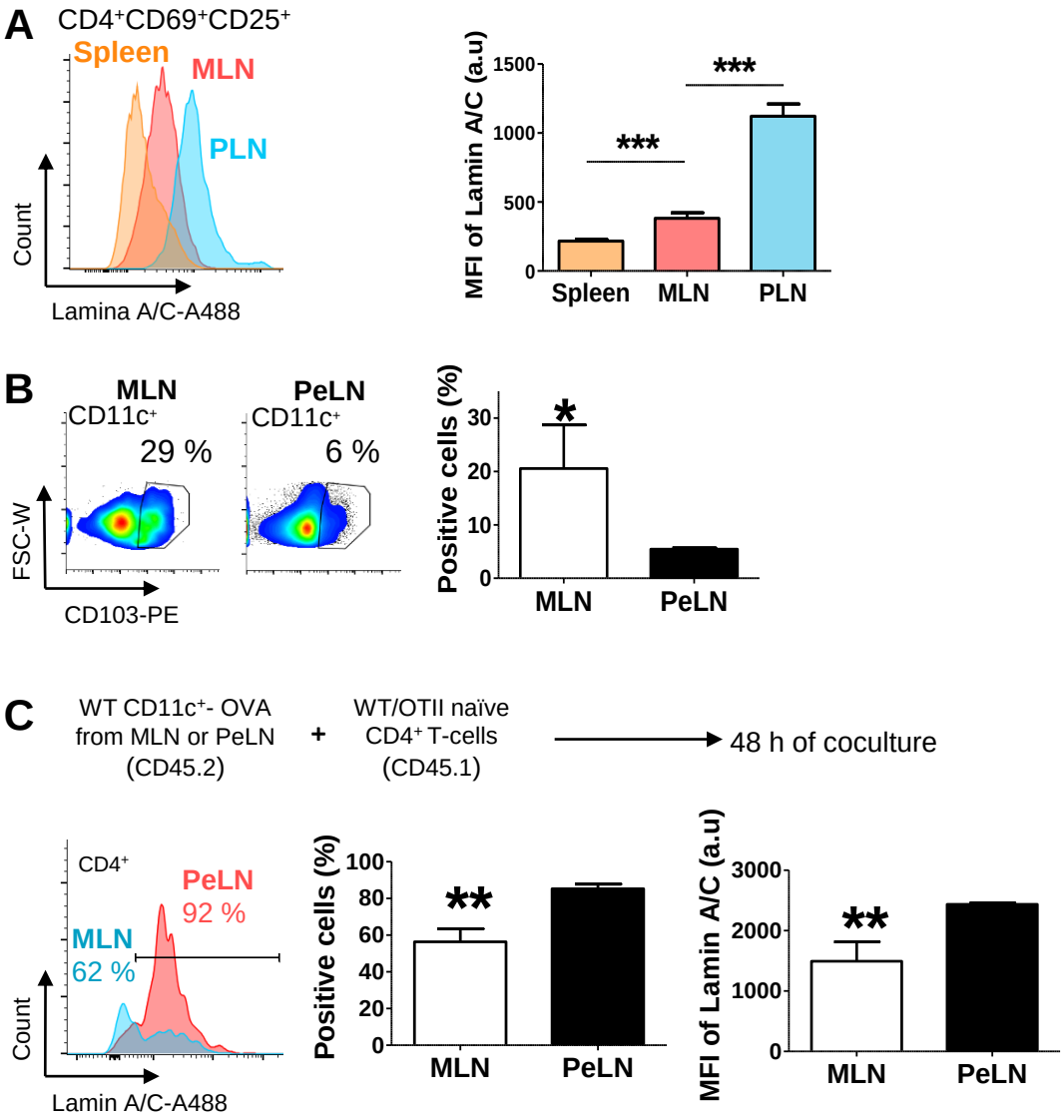
A
CD4+CD69+CD25+
Spleen
MLN
PLN
Count
Lamina A/C-A488
MFI of Lamin A/C (a.u)
1500
1000
500
0
***
***
Spleen
MLN
PLN
B
MLN
CD11c+
29 %
PeLN
CD11c+
6 %
FSC-W
CD103-PE
Positive cells (%)
30
20
10
0
*
MLN
PeLN
C
WT CD11c+- OVA
from MLN or PeLN
(CD45.2)
+
WT/OTII naïve
CD4+ T-cells
(CD45.1)
48 h of coculture
CD4+
PeLN
92 %
MLN
62 %
Count
Lamin A/C-A488
Positive cells (%)
100
80
60
40
20
0
**
MLN
PeLN
MFI of Lamin A/C (a.u)
3000
2000
1000
0
**
MLN
PeLN

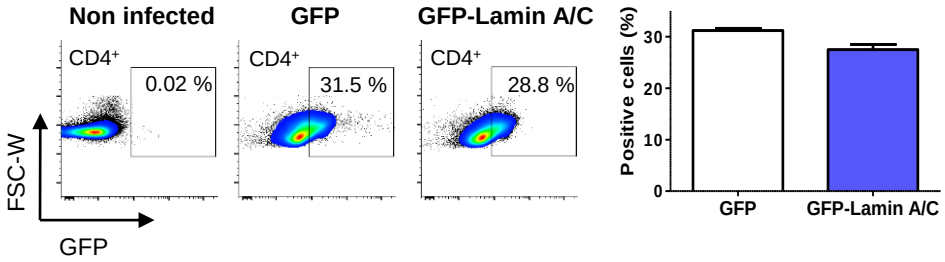
Non infected
GFP
GFP-Lamin A/C
CD4+
0.02 %
CD4+
31.5 %
CD4+
28.8 %
FSC-W
GFP
Positive cells (%)
30
20
10
0
GFP
GFP-Lamin A/C

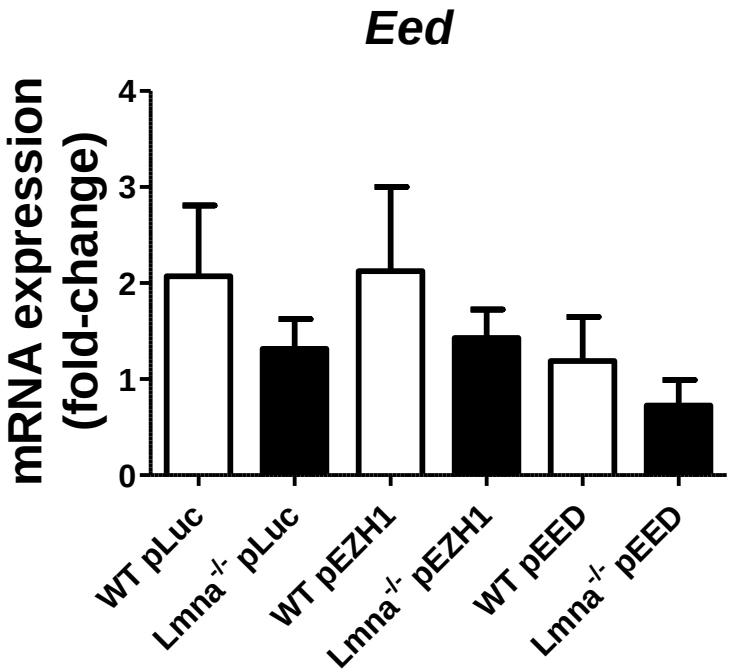
Eed
mRNA expression
(fold-change)
0
1
2
3
4
WT pLuc
Lmna-/- pLuc
WT pEZH1
Lmna-/- pEZH1
WT pEED
Lmna-/- pEED

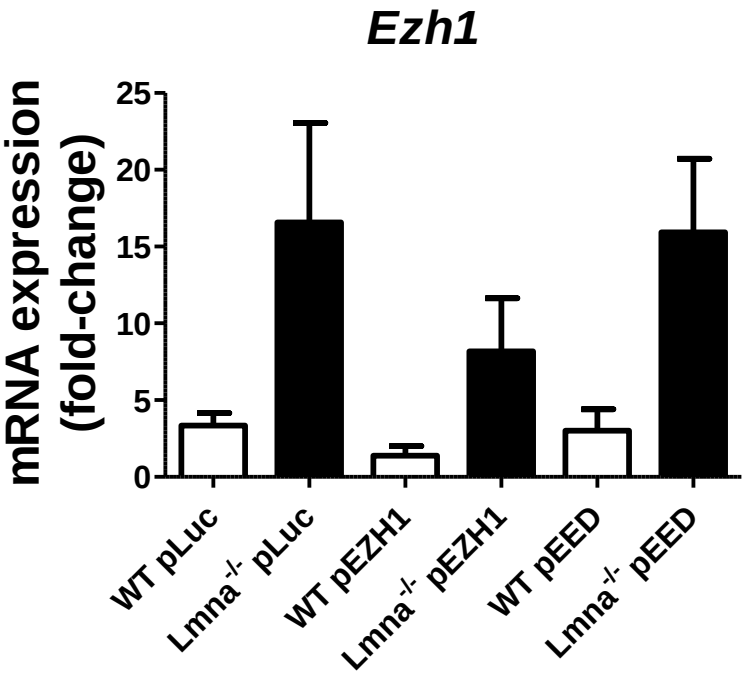
Ezh1
mRNA expression
(fold-change)
0
5
10
15
20
25
WT pLuc
Lmna-/- pLuc
WT pEZH1
Lmna-/- pEZH1
WT pEED
Lmna-/- pEED

A

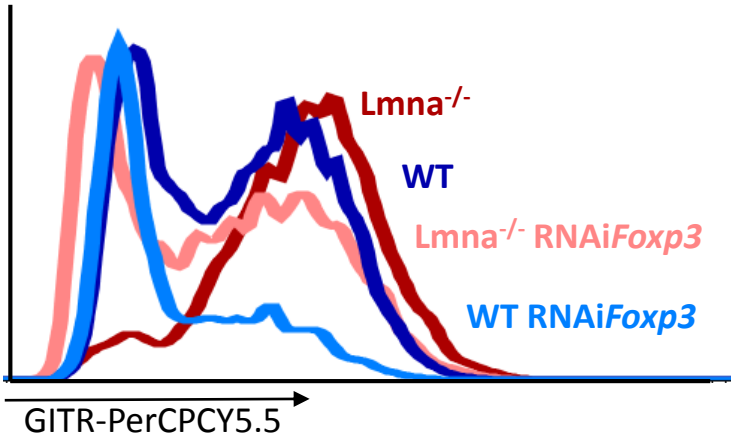
Lmna-/-
WT
Lmna-/- RNAiFoxp3
WT RNAiFoxp3
GITR-PerCPCY5.5

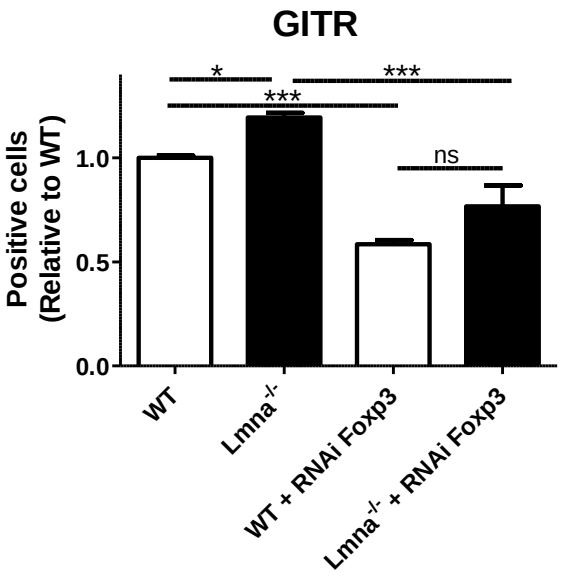
GITR
Positive cells (Relative to WT)
0.0
0.5
1.0
*
***
***
ns
WT
Lmna-/-
WT + RNAi Foxp3
Lmna-/- + RNAi Foxp3

B

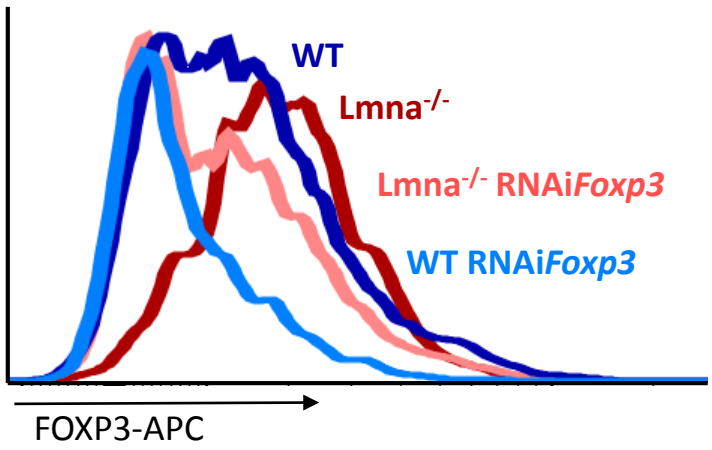
WT
Lmna-/-
Lmna-/- RNAiFoxp3
WT RNAiFoxp3
FOXP3-APC

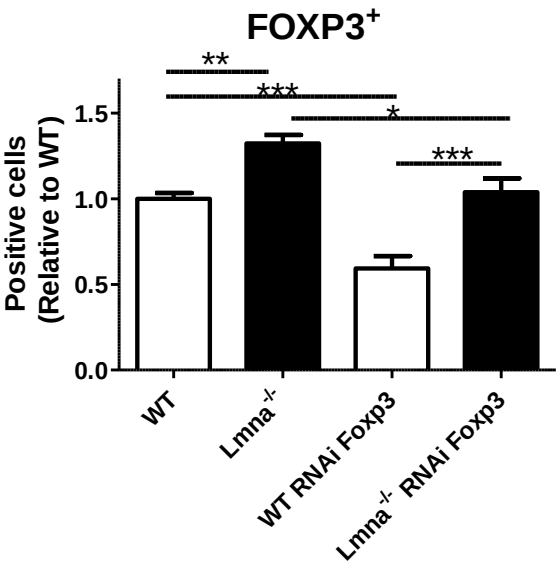
FOXP3+
Positive cells (Relative to WT)
0.0
0.5
1.0
1.5
**
***
*
***
WT
Lmna-/-
WT RNAi Foxp3
Lmna-/- RNAi Foxp3

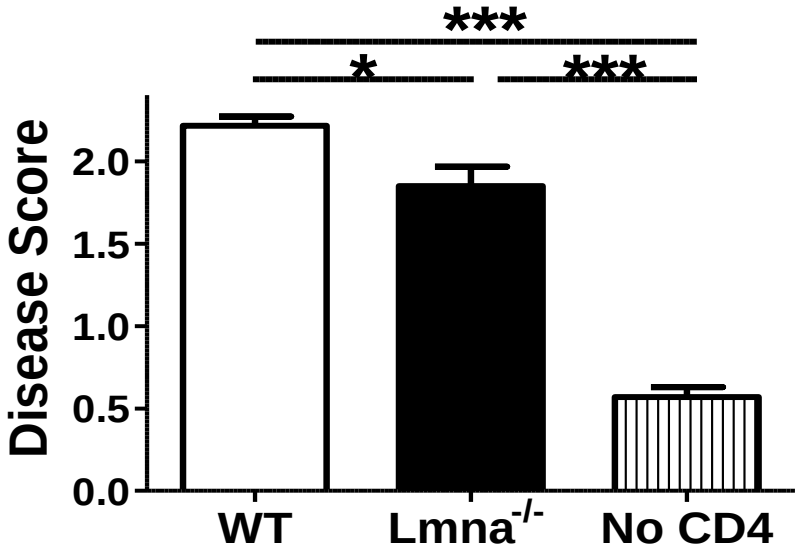
***
*
***
Disease Score
2.0
1.5
1.0
0.5
0.0
WT
Lmna-/-
No CD4

A

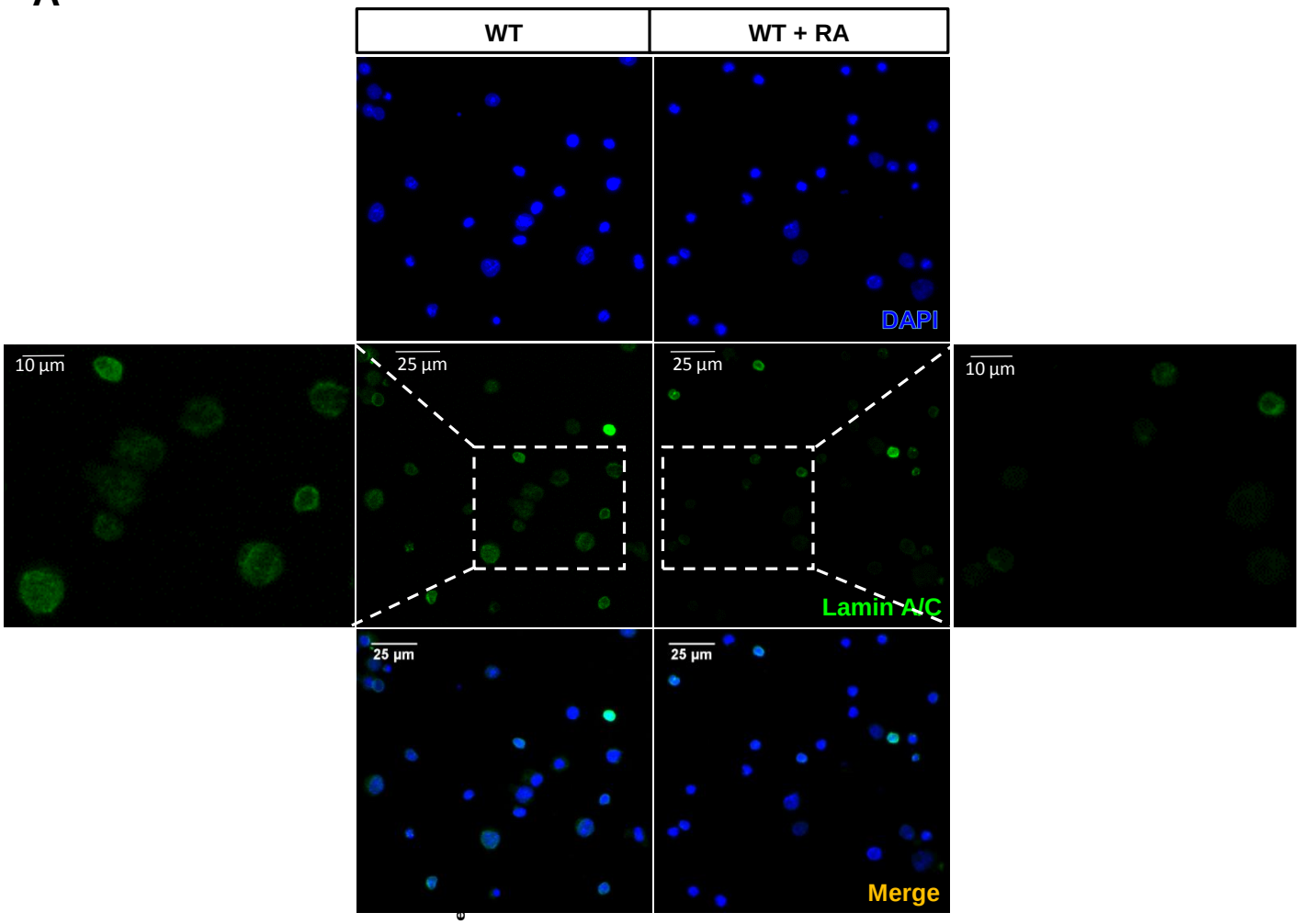
WT
WT + RA
DAPI
10 µm
25 µm
25 µm
10 µm
Lamin A/C
25 µm
25 µm
Merge

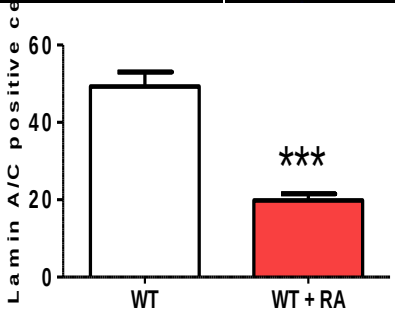
Lamin A/C positive ce
60
40
20
0
***
WT
WT + RA

B

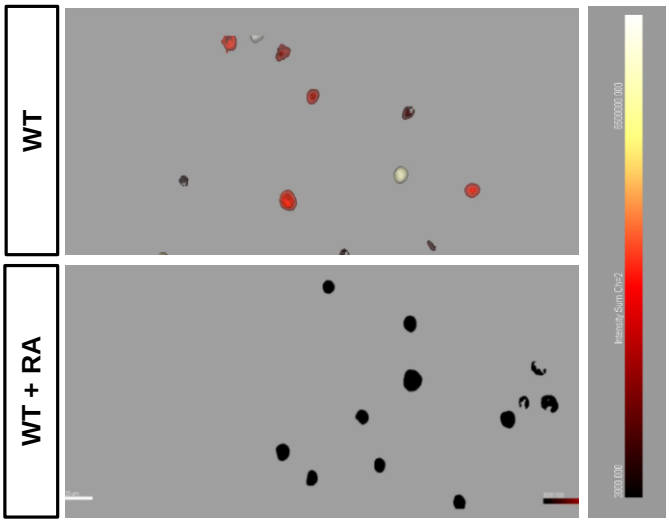
WT
WT + RA
High
Low

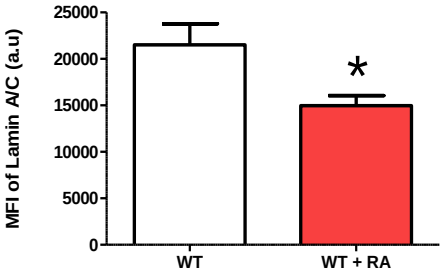
MFI of Lamin A/C (a.u)
25000
20000
15000
10000
5000
0
*
WT
WT + RA

A

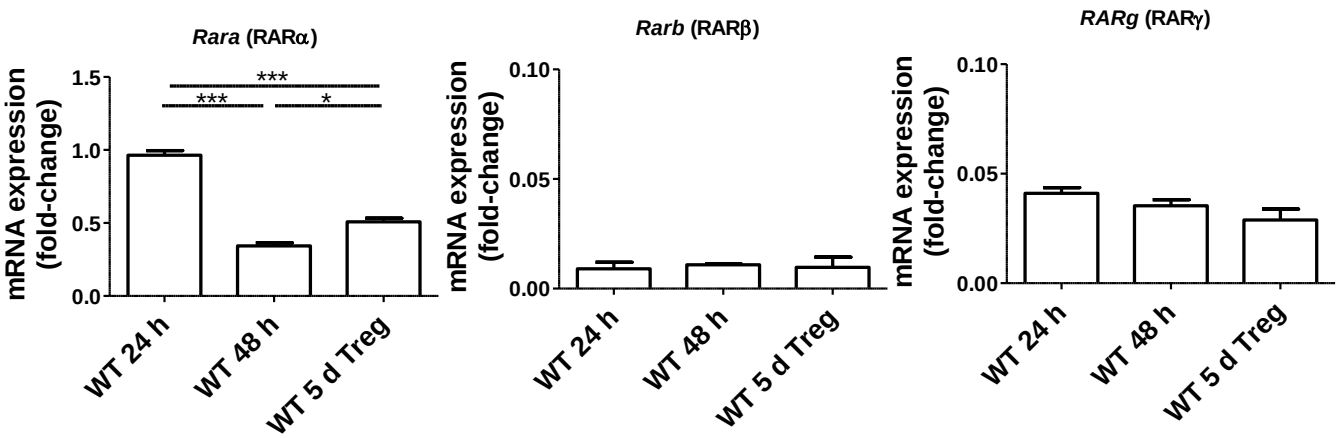
Rara (RARα)
Rarb (RARβ)
RARg (RARγ)
mRNA expression (fold-change)
1.5
1.0
0.5
0.0
0.10
0.05
0.00
***
***
*
WT 24 h
WT 48 h
WT 5 d Treg

B

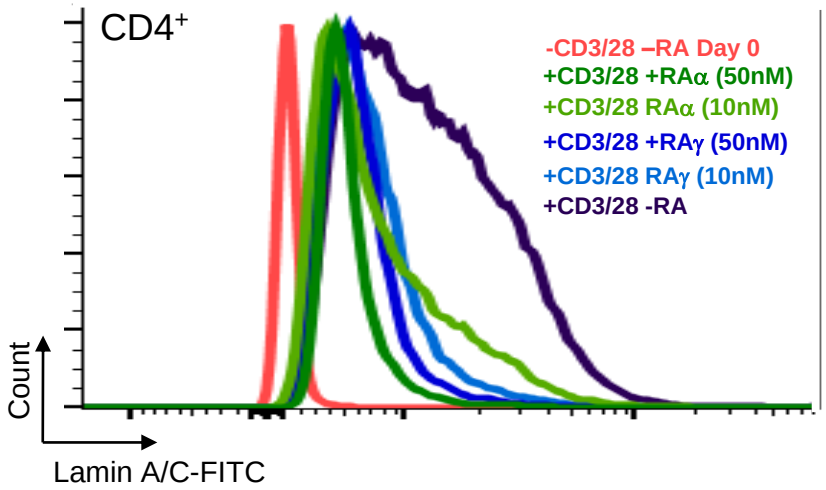
CD4+
-CD3/28 –RA Day 0
+CD3/28 +RAα (50nM)
+CD3/28 RAα (10nM)
+CD3/28 +RAγ (50nM)
+CD3/28 RAγ (10nM)
+CD3/28 -RA
Count
Lamin A/C-FITC

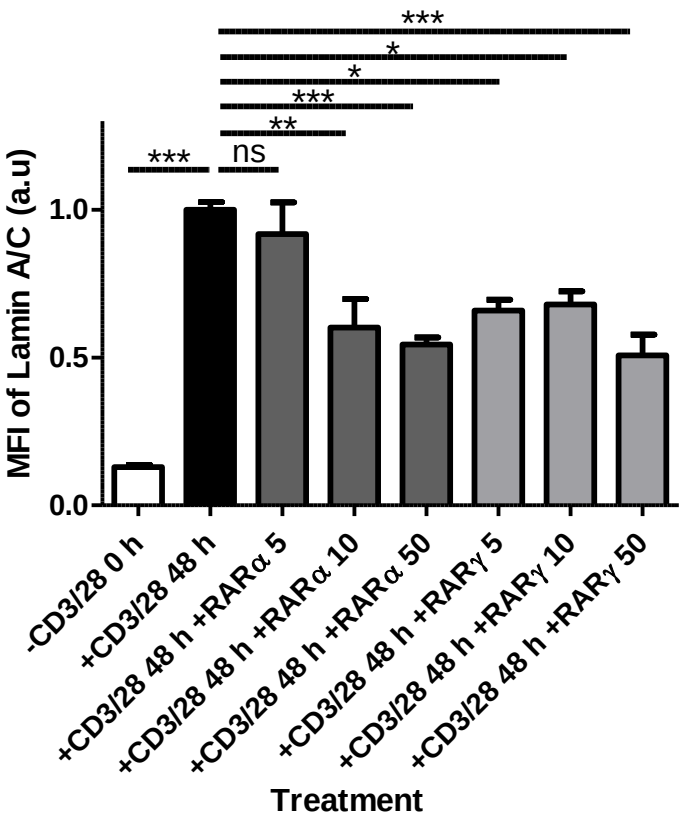
***
*
*
***
**
***
ns
MFI of Lamin A/C (a.u)
1.0
0.5
0.0
-CD3/28 0 h
+CD3/28 48 h
+CD3/28 48 h +RARα 5
+CD3/28 48 h +RARα 10
+CD3/28 48 h +RARα 50
+CD3/28 48 h +RARγ 5
+CD3/28 48 h +RARγ 10
+CD3/28 48 h +RARγ 50
Treatment

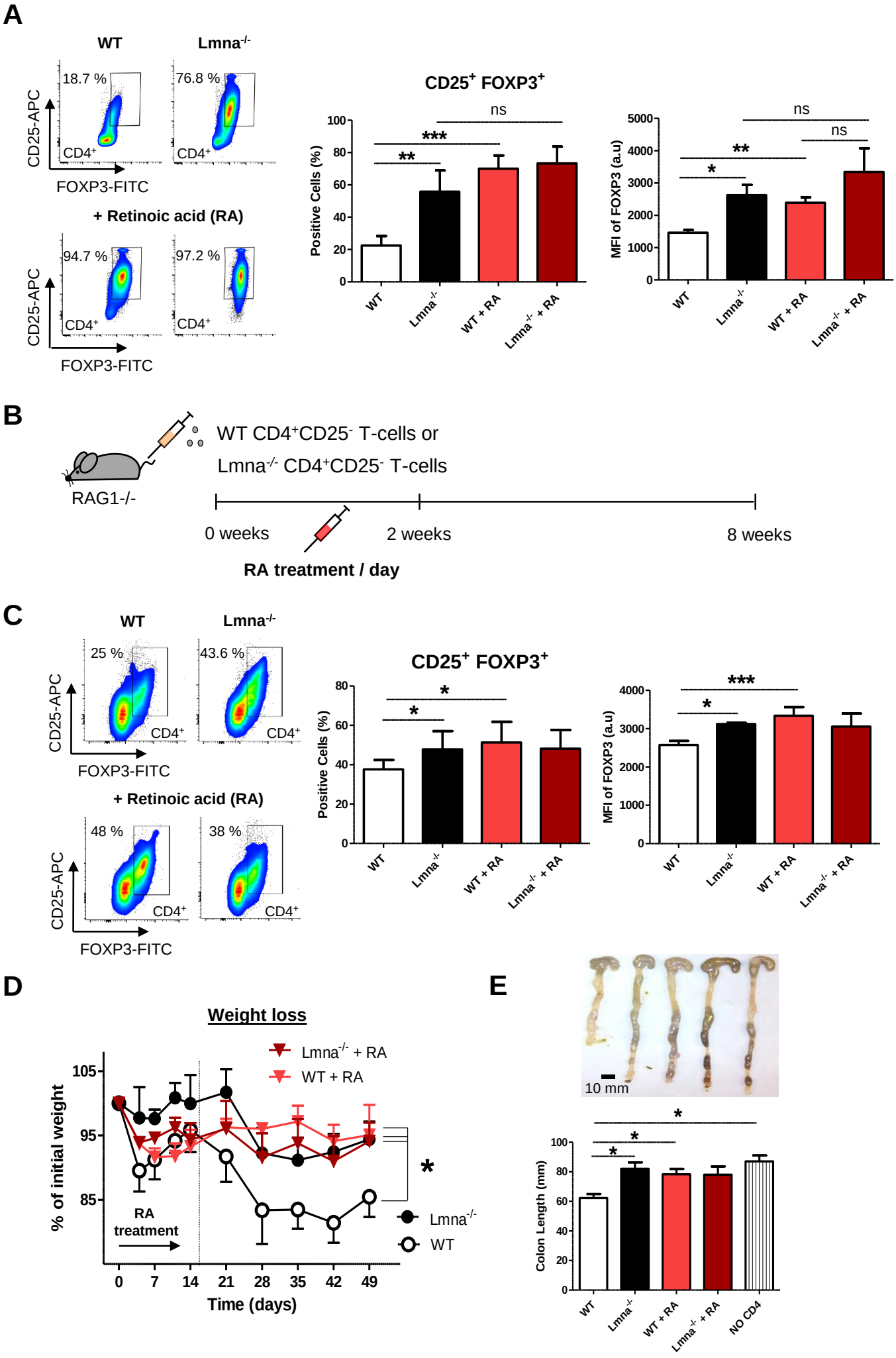
A
WT
Lmna-/-
18.7 %
76.8 %
CD4+
CD25-APC
FOXP3-FITC
+ Retinoic acid (RA)
94.7 %
97.2 %
CD25+ FOXP3+
Positive Cells (%)
MFI of FOXP3 (a.u)
ns
***
**
*
WT
Lmna-/-
WT + RA
Lmna-/- + RA
B
WT CD4+CD25- T-cells or
Lmna-/- CD4+CD25- T-cells
RAG1-/-
0 weeks
2 weeks
8 weeks
RA treatment / day
C
25 %
43.6 %
48 %
38 %
D
Weight loss
% of initial weight
RA treatment
Time (days)
E
10 mm
Colon Length (mm)
NO CD4

Supplemental Material and Methods

Mice

Lmna$^{-/-}$ mice have been described previously [69]. OTII and CD4-CRE mice were obtained from the Jackson Laboratory (stock number 004194 and 017336, respectively), as were C57BL/6J 129S7-Rag1tm1Mom/J (*Rag1*$^{-/-}$) mice, which lack B and T lymphocytes. Female mice were used from 8 to 12 weeks of age. C57BL/6-CD45.1^{+} and C57BL/6-CD45.1^{+} CD45.2^{+} *Lmna*$^{flox/flox}$ mice were kindly provided by Y. Zheng [70]. C57BL/6 CD4-CRE-*Lmna*$^{flox/flox}$ mice were generated by crossing C57BL/6-CD4-CRE and C57BL/6-*Lmna*$^{flox/flox}$ mice. Foxp3-IRES-mRFP (FIR) mice were obtained from Jackson Laboratory (stock number 008374) and were crossed with C57BL/6 CD4-CRE-*Lmna*$^{flox/flox}$ mice. All mice were bred in specific pathogen-free conditions at the *Centro Nacional de Investigaciones Cardiovasculares* (CNIC).

Animal experiments were approved by the local ethics committee and the Spanish Ministry of Agriculture and Fisheries, Food and Environment. All animal procedures conformed to EU Directive 86/609/EEC and Recommendation 2007/526/EC regarding the protection of animals used for experimental and other scientific purposes, enforced in Spanish law under Real Decreto 1201/2005.

Antibodies

Alexa Fluor 488-conjugated anti-lamin-A/C and Alexa Fluor 488-conjugated mouse immunoglobulin (Ig) G1 isotype control were obtained from Cell Signaling. Anti-CD3, anti-CD28, APC-conjugated anti-CD45.1, PECy7-conjugated anti-CD45.1, PE-conjugated anti-

IFNγ, APC-conjugated anti-IFNγ, FITC-conjugated anti-CD4, V450-conjugated anti-CD4, APC-conjugated anti-CD25, PECy7-conjugated anti-CD25, and FITC-conjugated anti-FOXP3 were from Tonbo Bioscience. PercpCy5.5-conjugated anti-CD64, PE-conjugated anti-CD103, Pe-Cy7-conjugated GITR, and FITC-conjugated anti-CD11c were from Biolegend. PE-conjugated anti-IL-10 and biotinylated antibodies against B220, CD19, MHCII, CD11c, CD11b, CD44, CD49b, IgM, CD25, and CD8α were from BD Biosciences. Antibodies against H3K4me3, H3K4me1, H3K27me3, and H3K27ac were from Diagenode.

Plasmids

The plasmids for retroviral transduction of control luciferase RNAi, EZH1 RNAi and EED RNAi were a gift from George Daley (pSMP-Luc: Addgene plasmid # 36394; http://n2t.net/addgene:36394; RRID: Addgene_36394. pSMP-EZH1_1: Addgene plasmid # 36359; http://n2t.net/addgene:36359; RRID: Addgene_36359. pSMP-EED_2: Addgene plasmid # 36386; http://n2t.net/addgene:36386; RRID: Addgene_36386) [71].

The plasmid for retroviral transduction of *Foxp3* RNAi was a gift from Dan Littman (LMP 1066, Addgene plasmid # 24071; http://n2t.net/addgene:24071; RRID: Addgene_24071) [72].

The plasmid for retroviral transduction of pBABE-puro-GFP-wt-lamin A (Addgene plasmid # 17662; http://n2t.net/addgene:17662; RRID: Addgene_17662) and pBABE-puro-GFP were a gift from Tom Misteli [73].

T-cell isolation, activation, and polarization

$CD4^+$ $CD25^-$ T-cells from spleens were purified by negative selection on separation columns (Miltenyi Biotec) after labeling the cells with a cocktail of biotinylated antibodies against

B220, CD19, MHCII, CD11c, CD11b, CD44, CD25, CD49b, IgM, and CD8α and a solution containing streptavidin-bound magnetic microbeads (Miltenyi Biotec). For polarizing experiments, $CD4^+$ $CD25^-$ T-cells from WT and $Lmna^{-/-}$ mice were stimulated with plate-bound anti-CD3 (10 μg/mL) and soluble anti-CD28 (2 μg/mL).

Polarizing conditions were as follows: TGF-β (20 ng/mL) and IL-2 (10 ng/mL) for Treg polarization, IL-23 (10 ng/mL) and IL-6 (20 ng/mL) for Th17 polarization and IL-12 (10 ng/ml) and IL-2 (10 ng/mL) for Th1 polarization. Antibodies were from BD bioscience and cytokines from Tonbo Bioscience. Cells were cultured for the indicated times in RPMI-1640 medium (GIBCO) supplemented with 10% fetal bovine serum (FBS), 2 mM ethylenediaminetetra-acetic acid (EDTA), 100 mg/mL penicillin, 100 mg/mL streptomycin, 20 mM 4-(2-hydroxyethyl)-1-piperazineethanesulfonic acid (HEPES), 55 μM β-2-mercaptoethanol, 1 mM sodium pyruvate, and 2 mM L-glutamine.

Quantitative proteomics

Proteins were extracted with 50 mM Tris-HCl, 2 % SDS, 50 mM iodoacetamide (IAA) and digested using the filter aided sample preparation (FASP) protocol with minor modifications [21]. For stable isobaric labeling, the resulting tryptic peptides were dissolved in 100 mM triethylammonium bicarbonate (TEAB) buffer, and each peptide sample was labeled using the 10-plex TMT Reagents (Thermo Fisher). To increase proteome coverage, TMT-labeled samples were fractioned by high-pH reverse-phase chromatography (High pH Reversed-Phase Peptide Fractionation Kit, Pierce). Labeled peptides were analyzed by LC-MS/MS in an Orbitrap Fusion mass spectrometer (Thermo Fisher). For peptide identification, the spectra were analyzed with Proteome Discoverer version 2.1.0.81 using SEQUEST-HT (Thermo Fisher). Peptide identification at 1 % FDR was validated and quantitative data

analyzed using the WSPP statistical model [22]. Functional protein analysis of the whole set of quantified proteins was performed using the systems biology triangle algorithm (SBT) [23].

Inflammatory bowel disease mouse model

Intestine inflammation was induced by the inoculation of $\geq 5\times10^5$ $CD4^+$ $CD25^-$ T-cells from CD4-$CRE^{tg/wt}$-*Lmna*$^{flox/flox}$ or CD4-$CRE^{wt/wt}$-*Lmna*$^{flox/flox}$ mice into T-cell and B-cell immunodeficient *Rag1*$^{-/-}$ mice through the retro-orbital sinus [16, 17]. Mice were monitored over 8 weeks to assess colitis development. Body weight and symptoms were checked twice a week. Disease severity was assigned a clinical score as follows:

- Weight loss: 0 (no loss), 1 (1–5 %), 2 (5–10 %), 3 (10–20 %), and 4 (> 20 %).
- Stool consistency: 0 (normal), 2 (loose stool), and 4 (diarrhea).
- Rectal prolapse: 0 (absent), 2 (low), and 4 (pronounced).
- Rectal bleeding: 0 (absent), and 4 (present).
- Spine curvature: 0 (absent), 2 (low), and 4 (pronounced).

Histopathological analysis

After 8 weeks of IBD development, mouse colons were collected and fixed in 4 % paraformaldehyde for 48 h and transferred to 70 % ethanol. Colons were cut into six portions of approximately 5 mm. A set of three portions - one each from the proximal, medial, and distal colon - was dehydrated to xylene and embedded in paraffin. The remaining portions were used for mRNA expression analysis. Transverse colon sections (5 µm) were cut and stained with hematoxylin-eosin to evaluate inflammation severity. Images were obtained with an Olympus BX41 microscope. For each colon region, two images were evaluated on serial sections cut with a 100 µm separation (6 images per mouse). Colitis severity was

assessed according to the following features: leukocyte infiltration, goblet cell depletion, epithelial hyperplasia, crypt damage, and submucosal inflammation, with each feature assigned a score from 0 to 4. Ulceration was also scored as follows: 0 (absent), 2 (present), and 4 (prominent). Features were scored by two blinded observers, and were summed to give a final histological score.

In vitro Treg suppression assay

$CD4^+$ $CD25^-$ T-cells were isolated from CD4-$CRE^{tg/wt}$-*Lmna*$^{flox/flox}$ and CD4-$CRE^{wt/wt}$-*Lmna*$^{flox/flox}$ mice spleens and polarized toward Treg phenotype. After 6 days of *in vitro* differentiation, $CD4^+$ $CD25^-$ T-cells were isolated from CD45.1/WT mouse spleens, and Treg polarization was checked by flow cytometry. *In vitro*-generated Tregs were stained with FITC-conjugated anti-CD4, APC-conjugated anti-CD25, and 4',6-diamidine-2'-phenylindole dihydrochloride (DAPI) (Thermo Fisher) and selected by fluorescence-activated cell sorting (FACS). CD45.1/WT $CD4^+$ $CD25^-$ T-cells were stained with CellTrace Violet (Thermo Fisher). Treg:T-naïve cocultures then set up serial ratios (1:2, 1:4, 1:8, 1:16, 1:32, 0:1) in the presence of soluble anti-CD3 (10 μg/mL) and soluble anti-CD28 (2 μg/mL).

Retinoic acid (RA) treatment *in vitro* and *in vivo*

RA powder (ATRA, Sigma-Aldrich) was diluted in dimethyl sulfoxide (DMSO) and added to *in vitro* cultures at day 0 in a final concentration of 10 nM. After 48 h of incubation, RA was washed out. The RARα agonist BMS753 (Tocris) and the RARγ agonist CD1530 (Tocris) were diluted in DMSO and added to a final concentrations of 5, 10 or 50 nM for 48 h. Non-treated controls cells were cultured under the same conditions in the presence of DMSO.

For *in vivo* treatment, mice received intraperitoneal (i.p). injections of 30 µg/mL RA diluted in corn oil (Sigma-Aldrich) every day during the first 2 weeks of IBD induction in the mouse model.

Colon lymphocyte isolation

Colons were extracted from mice with induced IBD and washed with HBSS buffer (Thermo Fisher) supplemented with 100 mg/mL penicillin and 100 mg/mL streptomycin. Colons were then cut longitudinally and placed in HBSS containing 100 mg/mL penicillin and 100 mg/mL streptomycin, and 5mM 1.4 dithiothreitol (DTT) (Sigma-Aldrich) and incubated for 20 min at room temperature (RT) to break down the intestinal mucus. After, colons were washed and incubated again with HBSS and 2 mM EDTA during 20 min at 37 ºC to detach the intestinal epithelium. The colons were washed again, cut into small pieces, and incubated for 30 min at 37 ºC in HBSS supplemented with 100 mg/mL penicillin, 100 mg/mL streptomycin, 1 % type IV collagenase (Roche), and 10 mM DNase I (Sigma-Aldrich). The dispersed cell suspension was filtered through a 70 µm cell strainer, and the filtered cells were centrifuged at 1500 rpm for 5 min at 4 °C to obtain a cell pellet.

DC and $CD4^+$ T-cell *in vitro* cocultures

MLNs and PeLNs were isolated from CD45.2/WT mice, cut into small pieces, and incubated for 10 min at 37 ºC in HBSS containing 1 % liberase TL (Roche) and 1000 U/mL DNase I. The resulting cell suspension was filtered through a 70 µm cell strainer, and the filtered cells were centrifuged at 1800 rpm for 5 min at 4 ºC. The pelleted cells were stained with the following antibodies and reagents: FITC-conjugated anti-CD11c, PercpCy5.5-conjugated anti-CD64, PE-conjugated anti-CD103, and DAPI. Two DCs populations were selected by FACS: CD11c $CD64^-$ $CD103^+$ and CD11c $CD64^-$ $CD103^-$. Naïve $CD4^+$ T-cells were isolated

from CD45.1/OTII/WT mouse spleens, and DCs and naïve T-cells were cocultured at a 1:5 ratio.

Chromatin immunoprecipitation-quantitative PCR

$CD4^+$ $CD25^-$ T-cell pellets (2×10^6) were crosslinked according the protocol of Oldenburg and Collas [24], snap frozen, and preserved at -80 ºC. Crosslinked pellets were analyzed by chromatin immunoprecipitation (ChIP)-qPCR [24]. The amplification conditions were as follows: denaturation at 95 °C for 3 min; 40 cycles of 95 °C for 10 s, annealing at 60 °C for 15 s, extension at 72 °C for 20 s; and denaturation at 95 °C for 1 min. The primers used for ChIP-qPCR are listed in Supplementary Table 1, and were designed with the NCBI primer-designing tool using gene sequences obtained from the NCBI database. Promoter regions of the studied genes were selected by tracking backwards from the transcription start site (TSS) to the beginning of the gene sequence. The expression of each studied gene was analyzed by the comparative Ct method with Biogazelle qBasePLUS software, using the housekeeping genes *Ube2b* and *Gapdh* as internal controls. Results are presented as fold-change relative to control conditions.

Production of retrovirus and retroviral transduction

Phoenix-Eco retrovirus producer cell line were kindly provided by Dr. Daniel Martín Pérez (Viral Vector Unit of CNIC). Calcium phosphate-mediated DNA transfection was performed as previously described by Wigler, M *et al* [74] with some modifications. Briefly, the day before plasmid transfection, Phoenix-Eco cells were plated at a density of 2.5×10^6 cells per 10-cm dish in DMEM medium (GIBCO) supplemented with 10 % FBS, 100 mg/mL penicillin, and 100 mg/mL streptomycin. The next day, cells were transfected with 5 μg viral vector. Plasmid DNA was mixed with HBSS buffer, then 1 M $CaCl_2$ was added and the mixture was allowed to stand at RT for 15 min. Finally, the mixture was added to the plates

in a dropwise manner. After 16 hours, media were aspirated, and cultures were fed with fresh DMEM medium supplemented with 10 % FBS, 100 mg/mL penicillin, and 100 mg/mL streptomycin. 48 h after transfection, viral supernatants were collected and filtered through 45 μm pore size filters.

For viral transduction, isolated naïve $CD4^+$ T-cells were activated for 24 h before the addition of fresh viral supernatants. Cells were then spun for 90 min at 2200 rpm at 30 ºC . After spin infection, the cells were cultured in fresh RPMI-1640 medium and harvested on day 5 for intracellular staining and RNA analysis through Reverse transcription quantitative PCR (RT-qPCR).

Reverse transcription-quantitative PCR

Total RNA was isolated with TRI Reagent™ Solution (Invitrogen-Thermo Fisher) and isopropanol precipitation or with the RNeasy Mini kit (Qiagen). RNA concentration and purity were assessed from the ratio of absorbance at 260 and 280 nm. Complementary DNA (cDNA) was synthesized from total RNA (0.1 to 1 μg per reaction) with the High Capacity cDNA Reverse Transcription Kit (Applied Biosystems) using random primers and RNase Inhibitor. Quantitative PCR was performed in technical triplicates with the ABI PRISM 7900HT Sequence Detection System (Applied Biosystems) and using the PCR Power SYBR Green PCR Master Mix (Applied Biosystems). The amplification conditions were as follows: denaturation at 95 °C for 10 min; 40 cycles of 95 °C for 15 s, annealing at 60 °C for 30 s, extension at 72 °C for 40 s; and denaturation at 95 °C for 1 min, followed by dissociation curve analysis. Primer sequences are listed in Supplementary Table 2. The results were analyzed as is indicated above, using the housekeeping genes *Hprt1* (hypoxanthine phosphoribosyl transferase 1), *Actb* (β-actin) and *Gapdh* as internal controls. Results are presented as fold-change relative to internal controls.

Flow cytometry

$CD4^+$ T-cells were stimulated for 6 h with PMA (20 ng/mL) plus ionomycin (1µg/mL). Brefeldin A (Sigma-Aldrich) was added for the last 2 hours to allow intracellular cytokine accumulation. Surface antigens were stained with antibodies, and cells were then fixed and permeabilized with either the Cytofix or the Cytoperm kit (BD Biosciences), followed by staining of intracellular cytokines and transcription factors. FOXP3 was stained using the Mouse Foxp3 Buffer set (BD Biosciences). For lamin A/C intranuclear staining, cells were permeabilized by incubation with 0.5 % Triton X-100 for 5 min. The antibodies were used at the manufacturer-recommended concentrations. Data were acquired in FACSCantoII or LSRFortessa flow cytometers (BD Biosciences) and were analyzed with BD FACSDIVA (BD Biosciences) or FlowJo (Treestar Inc.) software.

Immunofluorescence and microscopy

$CD4^+$ T-cells were plated for1 h at 37 ºC onto Poly-L-Lysine-coated slides (50 µg/mL; Sigma-Aldrich). Samples were then fixed with 4 % paraformaldehyde and permeabilized with 0.5 % Triton X-100/PBS solution for 5 min at room temperature. Cells were incubated with Alexa488-conjugated anti-mouse lamin A/C (1:100, Cell Signaling) and DAPI (1:500, Thermo Fisher) for 1 hour at room temperature.

Samples were mounted in Fluoromount-G imaging medium, and immunofluorescence images were acquired with a Zeiss LSM700 confocal microscope (Plan-Apochromat 63 × 1.4, 40 × 1.3, 25 × 1.2 oil objective; Carl Zeiss, Oberkochen, Germany). Images were analyzed using ImageJ Fiji software and Imaris software (Bitplane) by an observer blinded to genotype.

Statistical analysis

Statistical analyses were performed with Prism GraphPad or Microsoft Office Excel. Unless otherwise stated, statistical significance was calculated by two-tailed Student *t*-test. When specified, one-way ANOVA or 2-way ANOVA with Bonferroni post-hoc multiple comparison test was used. Significance of differences was calculated as follows: *P < 0.05, **P < 0.01, ***P < 0.001, and **** P < 0.0001.

Citation numbers refer to the main manuscript.

Supplementary figure legends

Supplementary Figure 1. GFP-lamin A/C retrovirus drives lamin A/C overexpression. Splenocytes were isolated from CD45.1 WT/OTII mice and CD45.2 Lmna$^{-/-}$/OTII mice and cocultured *in vitro* in the presence of OVA-peptide for 48 h. The splenocytes were then transfected with GFP or GFP-lamin A/C retrovirus and cultured *in vitro* with cytokines to promote Treg differentiation. Representative plots are shown of GFP^{+} transfected splenocytes; the graph shows quantification (n = 3 and 3 mice). Data are means ± SEM of one representative experiment of 3 analyzed by the Student *t*-test. ns, not significant.

Supplementary Figure 2. Lmna$^{-/-}$ CD4^{+} T-cells show increased *Ezh1* and reduced *Eed* mRNA levels RT-qPCR analysis of *Eed,* and *Ezh1* mRNA expression in CD4^{+} T-cells isolated from WT and *Lmna*$^{-/-}$ mouse spleens, activated *in vitro* with anti-CD3/CD28 for 48 h (n = 6 mice) and retroviral transduced with a scramble RNAi (pLuc), a EED RNAi (pEED) or a EZH1 RNAi (pEZH1). Upon transduction, cells were incubated for 72 hours in the presence of cytokine IL-12 and IL-2 to promote Th1 differentiation. Data are means ± SEM

of 3 independent experiments analyzed by one-way ANOVA with the Bonferroni multiple comparison test.

Supplementary Figure 3. FOXP3 downregulation reduces GITR membrane expression in Lmna$^{-/-}$ and WT CD4^{+} T-cells.

Naïve CD4^{+} T-cells were isolated from WT and *Lmna*$^{-/-}$ mouse spleens and stimulated with anti-CD3/CD28 antibodies for 2 days and differentiated in the presence of cytokines TGF-β and IL-2 to promote Treg phenotype. At day 2, activated cells were retroviral transduced with a RNAi against *Foxp3*. Plots and graphs show **(A)** GITR and **(B)** FOXP3 positive cells as a value relative to control transduced WT cells (n = 6-9 pools from at least 2 mice). Data are means ± SEM analyzed by one-way ANOVA with the Bonferroni multiple comparison test. *P < 0.05, **P < 0.01, ***P < 0.001.

Supplementary Figure 4. A-type lamin deficiency in CD4^{+} T-cells protects against IBD development in mice. *Rag1*$^{-/-}$ mice were adoptively transferred with WT or *Lmna*$^{-/-}$ CD4^{+} CD25^{-} T-cells to induce IBD. Mice were sacrificed 8 weeks after T-cell transfer. **(E)** The graph shows the quantification of the representative micrographs of hematoxylin-eosin stained colon sections of figure 4. The graph shows the disease score (0-3) recapitulating markers of intestinal inflammation indicated on the micrograph: leukocyte infiltration (1), goblet cell depletion (2), epithelial hyperplasia (3), crypt damage (4), and submucosal inflammation (5) (n = 6-7, at least 6 mice from a representative experiment of 5). Data are

means ± SEM analyzed by one-way ANOVA with the Bonferroni multiple comparison test. *P < 0.05;**P < 0.01;***P < 0.001. Black *: comparison between WT and *Lmna*$^{-/-}$.

Supplementary Figure 5. Retinoic acid (RA) downregulates lamin A/C expression in CD4^{+} T-cells. Naïve CD4^{+} T-cells were isolated from WT mouse spleens and activated with anti CD3/CD28 antibodies for 2 days in the presence of retinoic acid (RA, ATRA) or vehicle. **(A)** Immunofluorescent labeling of the nuclear envelope protein lamin A/C (green) in 48 h-activated CD4^{+} T-cells counterstained with DAPI (blue). Scale bars, 25 µm in main views and 10 µm in the high-magnification views of the boxed areas. The graph shows the percentage of lamin A/C expressing cells. **(B)** Representative volume and intensity analysis of lamin A/C staining (n = 6, 6 samples of 3 pools of 2 mice). Data are means ± SEM analyzed by unpaired Student *t*-test. *P < 0.05; ***P < 0.001.

Supplementary Figure 6. Expression of retinoic acid receptor α, β, and γ in naïve, activated and Treg differentiated CD4 T cells and stimulation of RARα or RARγ reduces lamin A/C protein induction upon CD4 T cell stimulation.

(A) Naïve CD4^{+} T-cells were isolated from WT and *Lmna*$^{-/-}$ mouse spleens and stimulated with anti-CD3/CD28 antibodies for 5 days in the presence of cytokines TGF-β and IL2 to trigger Treg differentiation. RT-qPCR analysis of *Rara* (RARα), *Rarb* (RARβ), and *Rarg* (RARγ) mRNA expression. Data are means ± SEM of at 3 independent experiments analyzed by one-way ANOVA with the Bonferroni multiple comparison test. (B) Naïve CD4^{+} T-cells were isolated from WT mouse spleens and activated with anti CD3/CD28 antibodies for 2 days in the presence of RARα or RARγ agonist or vehicle. The plot and the graph show the lamin A/C mean fluorescence intensity (MFI) analysis by flow cytometry of CD4^{+} T-cells.

Supplementary Figure 7. Lamin A/C downregulation augments Treg differentiation *in vitro* and *in vivo* and provides equal protection against IBD as retinoic acid (RA) treatment. (A) Naïve $CD4^+$ T-cells were isolated from WT and *Lmna*$^{-/-}$ mouse spleens and stimulated with anti CD3/CD28 antibodies in the presence of RA or vehicle for 48 h, when Treg cytokines were added. Representative plots show the percentage of $CD25^+$ $FOXP3^+$ Tregs in the $CD4^+$ T-cell population analyzed by flow cytometry at day 5 of Treg differentiation. Graphs show quantification of the $CD25^+$ $FOXP3^+$ Treg percentage and FOXP3 MFI (n = 6, 6 mice). **(B)** *Rag1*$^{-/-}$ mice were adoptively transferred with WT or *Lmna*$^{-/-}$ $CD4^+$ $CD25^-$ T-cells to induce IBD development. During the first 2 weeks, mice received daily i.p injections of RA. Mice were sacrificed 8 weeks after the T-cell transfer. **(C)** Flow cytometry analysis of $CD25^+$ $FOXP3^+$ cells in MLNs at 8 weeks after T-cell transfer. **(D)** Weight loss during IBD development. **(E)** Representative colons and quantification of colon length (mm) after 8 weeks of IBD (n = 5-9, at least 5 mice of a representative experiment of 2). Data are means ± SEM analyzed by 1-way ANOVA (A, B, D, F) and 2-way ANOVA (E) with the Bonferroni multiple comparison test. *P < 0.05; **P < 0.01; ***P < 0.001.

Supplementary tables

Supplementary Table 1. Primers used for ChIP-qPCR analysis

Gene	5'-3' Forward sequence	5'-3' Reverse sequence
Tbx21 (T-bet)	CCGTAGTTATTGGAATAGAACA	ATACCAACCGGTGTCTGTGT
Foxp3	CCCAGGAGGCCATTAACAGG	TTTGGCCCCATGCTATGGTT
Rorc (RORγt)	AGCTGCTTGGCTCAGCATAA	TTGCCTGCGTCATTCTGACT
Ube2b	TCACGTGACCTGCTCTGATG	GCATCCGGAGCCTGAGATTT
Gapdh	GTTGCACTGGCCTAGCAAAG	GACCGGGATTCTTCACTCCG

Supplementary table 2. Primers used for RT-qPCR analysis

Gene	5'-3' Forward sequence	5'-3' Reverse sequence
Tbx21 (T-bet)	GAAAGGCAGAAGGCAGCAT	GAGCTTTAGCTTCCCAAATGA
Foxp3	CTCGTCTGAAGGCAGAGTCA	TGGCAGAGAGGTATTGAGGG
Ifng (IFNγ)	TGGCTCTGCAGGATTTTCAT	TCAAGTGGCATAGATGTGGAA
Il12a (IL-12)	CTGCTTGACTCTGACATCT	CCACTGCTGACTAGAACTC
Tgfb1 (TGFβ)	ACCATGCCAACTTCTGTCTG	CGGGTTGTGTTGGTTGTAGA
Ebi3 (IL-35)	CTTACAGGCTCGGTGTGGC	GTGACATTTAGCATGTAGGGC
Il10	CCCTTTGCTATGGTGTCCTT	TGGTTTCTCTTCCCAAGACC
Il17a (IL-17)	AGAATTCATGTGGTGGTCCA	ACTACCTCAACCGTTCCACG
Rocg (RORγt)	GGTGACCAGCTACCAGAGG	AGCTCCATGAAGCCTGAAAG
Il23a (IL-23)	CAACTTCACACCTCCCTAC	CCACTGCTGACTAGAACT
Il6	GACAAAGCCAGAGTC	CTAGGTTTGCCGAGTAGATCT
Il22	CCGAGGAGTCAGTGCTAAG	CATGTAGGGCTGGAACCTGT
Hprt1	CCTAAGATGAGCGCAAGTTG	CCACAGGACTAGAACACCTGC
Gapdh	CTACACTGAGGACCAGGTTG	GGTCTGGGATGGAAATTGTG
Actb (β-actin)	GACGGCCAGGTCATCACTA	AGGAAGGCTGGAAAAGAGC
Icos	GCTCGGCCGATCATAGGATG	CCTCCACTAAGGTTCCTTTCTT
Tnfrsf18 (GITR)	CAAGGTTCAGAACGGAAGT	GAAGATGACAGTCAAATG
Ctla4	GCTTCCTAGATTACCCCTTCT	AGGTGCCCGTGCAGATGGAA
Pdcd1 (PD-1)	CGTCCCTCAGTCAAGAGGAG	GTCCCTAGAAGTGCCCAACA
Itga2 (CD49b)	CCGGGTGCTACAAAAGTCAT	GTCGGCCACATTGAAAAAGT

Lag3	TCACTGTTCTGGGTCTGGAG	GGTAAAGTCGCCATTGTCTC
Il2ra (CD25)	AACAACTGCAATGACGGAGA	CAGCTGGCCACTGCTACCTT
Lmna	TGAGTACAACCTGCGCTCAC	TGACTAGGTTGTCCCCGAAG
Rara (RARα)	GGCGAACTCCACAGTCTTAA	GCTGGGCAAGTACACTACGAA
Rarb (RARβ)	GGGGTATACCTGGTACAAAT	CAGCTGGGTAAATACACCACG
Rarg (RARγ)	CCCAAGGATGCTGATGAAA	GCCCTTTCTGCTCCCTTAGT
Ezh1	TGAAATCTGAGTATATGCGG	AGATATCCTGGCTGTCGAAC
Lbr	GTGCTCCTGAGTGCTTAC	GCCAATGAAGAAGTCGTAC
Eed	GCAACAGAGTAACCTTATAC	CAACTGCTAATAGAGGGTGG